Higher-order topological sensitivity for 2-D potential problems. Application to fast identification of inclusions

Marc Bonnet

Higher-order topological sensitivity for 2-D potential problems. Application to fast identification of inclusions

Marc BONNET

Solid Mechanics Laboratory (UMR CNRS 7649), Department of Mechanics
École Polytechnique, F-91128 Palaiseau cedex, France
bonnet@lms.polytechnique.fr

Abstract

This article concerns an extension of the topological derivative concept for 2D potential problems involving penetrable inclusions, whereby a cost function J is expanded in powers of the characteristic size ε of a small inclusion. The $O(\varepsilon^4)$ approximation of J is established for a small inclusion of given location, shape and conductivity embedded in a 2-D region of arbitrary shape and conductivity, and then generalized to several such inclusions. Simpler and more explicit versions of this result are obtained for a centrally-symmetric inclusion and a circular inclusion. Numerical tests are performed on a sample configuration, for (i) the $O(\varepsilon^4)$ expansion of potential energy, and (ii) the identification of a hidden inclusion. For the latter problem, a simple approximate global search procedure based on minimizing the $O(\varepsilon^4)$ approximation of J over a dense search grid is proposed and demonstrated.

1 INTRODUCTION

The sensitivity analysis of objective functions is nowadays based on well-established mathematical concepts, and provides very valuable computational tools for enhancing the performance and effectiveness of numerical methods for e.g. optimal design or inversion of experimental data. In its usual (but not mandatory) default acception, the term 'sensitivity' refers to first-order perturbation analyses with respect small variations of some feature of the system under consideration. Well-established methodologies for evaluating sensitivities of field variables or objective functions with respect to e.g. model parameters [1] or geometrical shapes [2] are available.

More recently, another sensitivity concept, namely that of topological sensitivity, appeared in [3, 4] in the context of topological optimization of mechanical structures. The aim of topological sensitivity is to quantify the perturbation of an objective function with respect to the nucleation of a small object $B_\varepsilon(\boldsymbol{a})$ of characteristic radius ε and given location $\boldsymbol{a}$, as a function of $\boldsymbol{a}$. If $J(\varepsilon;\boldsymbol{a})$ denotes

the value achieved by the objective function under consideration when $B_\varepsilon(\boldsymbol{a})$ is the only perturbation to an otherwise known reference medium, then in 2-D situations with Neumann or transmission conditions on $\partial B_\varepsilon(\boldsymbol{a})$ the topological derivative $\mathcal{T}_2(\boldsymbol{a})$ appears through an expansion of the form

$$J(\varepsilon;\boldsymbol{a}) = J(0) + \varepsilon^2 \mathcal{T}_2(\boldsymbol{a}) + o(\varepsilon^3)$$

Algorithms where "excess" material is iteratively removed according to the value of $\mathcal{T}_2(\boldsymbol{a})$ until a satisfactory shape and topology is reached have been formulated [5]. Other investigations have subsequently established the usefulness of the topological sensitivity as a preliminary sampling tool for inverse scattering problems, providing estimates of location, size and number of defects which can then (for example) be used as initial guesses in subsequent minimization-based inversion procedures [6, 7, 8, 9, 10, 11].

This article is concerned with an extension of the topological sensitivity concept whereby $J(\varepsilon;\boldsymbol{a})$ is expanded further in powers of ε. Specifically, the expansion to order $O(\varepsilon^4)$ for cost functions involving the solution of a 2-D potential problem on a domain containing a small object of size ε embedded in a medium occupying a domain of arbitrary shape is established. The chosen order $O(\varepsilon^4)$ stems from the fact that, for misfit functions J of least-squares format, the perturbations of the residuals featured in J are of order $O(\varepsilon^2)$ under the present conditions. The expansion will be found to have the form

$$J(\varepsilon;\boldsymbol{a}) = J(0) + \mathcal{T}_2(\boldsymbol{a})\varepsilon^2 + \mathcal{T}_3(\boldsymbol{a})\varepsilon^3 + \mathcal{T}_4(\boldsymbol{a})\varepsilon^4 + o(\varepsilon^4) \equiv J(0) + J_4(\varepsilon;\boldsymbol{a}) + o(\varepsilon^4) \qquad (1)$$

where coefficients $\mathcal{T}_2, \mathcal{T}_3, \mathcal{T}_4$ depend on the assumed characteristics of the small nucleating inclusion, namely its location $\boldsymbol{a}$, shape and constitutive characteristics (here the conductivity contrast). A similar approach, limited to impenetrable obstacles ($\beta = 0$), has been recently proposed in the context of the 3-D Helmholtz equation [12].

The concept of topological sensitivity, and higher-order topological expansions such as (1), are in fact particular instances of the broader class of asymptotic methods, where approximate solutions to problems involving inclusions in e.g. electromagnetic or elastic media and featuring a small geometrical parameter are sought in the form of expansions with respect to that parameter. A detailed presentation of such methods can be found in [13]. In this article, we are specifically interested in establishing computationally efficient methods for evaluating small-inclusion expansions of cost functions (rather than field variables) in the context of 2-D media edowed with a isotropic scalar conductivity. For that reason, and following common practice in usual sensitivity analyses as well as previous works on the topological derivative $\mathcal{T}_2$ [7, 14, 5, 11], an adjoint solution-based approach is chosen here as its obviates the need to evaluate higher-order sensitivities of field variables. Coefficients $\mathcal{T}_2, \mathcal{T}_3, \mathcal{T}_4$ are hence found in this article to be expressed in terms of the free and adjoint fields (i.e. the response of the reference medium to the applied and adjoint excitations), and also (for $\mathcal{T}_4$)

on the Green's function associated with the geometry and boundary condition structure under consideration. These expressions constitute the first main contribution of this article. A related study [15], restricted to the $O(\varepsilon^4)$ expansion of the potential energy for impenetrable nucleating inclusions, proposed inexact expressions for $\mathcal{T}_4$ [16, 17]. The missing terms in the $O(\varepsilon^4)$ expansion of [15] are pinpointed here on the basis of the present analysis.

The functions $\mathcal{T}_2(\boldsymbol{a}), \mathcal{T}_3(\boldsymbol{a}), \mathcal{T}_4(\boldsymbol{a})$ can be computed for sampling points $\boldsymbol{a}$ spanning a search grid at a computational cost which is of the order of a small number of forward solutions in the reference medium. This makes it possible to define a computationally fast approximate global search procedure, where the minimization of the polynomial approximant $J_4(\varepsilon; \boldsymbol{a})$ of the misfit function is performed for a large number of potential inclusion locations $\boldsymbol{a}$, whereas usual global search methods (e.g. evolutionary algorithms [18] or parameter-space sampling methods [19]) require large numbers of cost functions evaluations and are thus much more demanding. This fast approximate global search methodology, and the demonstration of its usefulness through numerical experiments on a inclusion identification problem, constitute the second main contribution of this article.

This article is organized as follows. Formulations and notation for the forward problems of interest and cost functions are reviewed in Section 2. Then, general expressions for coefficients $\mathcal{T}_2, \mathcal{T}_3, \mathcal{T}_4$ are established for a small inclusion of arbitrary shape and conductivity contrast buried in an arbitrary domain (section 5), based on a methodology whose main components are an adjoint-solution framework (Section 3) and an expansion of the total field on the inclusion boundary (Section 4). Simpler formulae are next obtained for the useful special case of a centrally-symmetric inclusion (section 5.2), leading to explicit formulae for a circular small inclusion (section 5.3). The generalization to several small inclusions is treated in section 6. Computational issues and links to other approaches are discussed in section 7. Finally, in section 8, numerical tests are performed on the $O(\varepsilon^4)$ expansion of potential energy, and a simple approximate global search procedure for hidden inclusion identification based on $J_4(\varepsilon; \boldsymbol{a})$ is next proposed and demonstrated on the same testing configuration.

2 FORWARD PROBLEM AND COST FUNCTIONS

Consider a reference configuration defined in terms of a two-dimensional domain Ω, either bounded or unbounded, with a sufficiently regular boundary S, and filled with a isotropic medium characterized by conductivity k.

2.1 Forward problem

Let $B^\star$ denote a trial penetrable object of isotropic conductivity $k^\star$, bounded by $\Gamma^\star$. Denoting by $\Omega^\star = \Omega \setminus (B^\star \cup \Gamma^\star)$ the region surrounding the inclusion, the application of prescribed potential u^{D} and flux p^{D} over S_{D} and S_{N}, respectively (where S_{N} and S_{D} are complementary disjoint subsets of

S) give rise to the potential $u^\star$ in $\Omega^\star$ and $B^\star$, governed by the field equations

$$\mathrm{div}(k\boldsymbol{\nabla}u^\star)=0 \ \ (\text{in } \Omega^\star), \qquad \mathrm{div}(k^\star\boldsymbol{\nabla}u^\star)=0 \ \ (\text{in } B^\star), \tag{2}$$

the boundary conditions

$$p^\star = p^{\mathrm{D}} \ \ (\text{on } S_{\mathrm{N}}), \qquad u^\star = u^{\mathrm{D}} \ \ (\text{on } S_{\mathrm{D}}) \tag{3}$$

(where $p^\star = k\boldsymbol{\nabla}u^\star\cdot\boldsymbol{n}$ denotes the flux through the external boundary, and with the unit normal $\boldsymbol{n}$ to S directed outwards of Ω) and the perfect-bonding transmission conditions

$$u^\star_{\mathrm{m}} = u^\star_{\mathrm{i}}, \quad (\boldsymbol{\nabla}u^\star)_{\mathrm{m}}\cdot\boldsymbol{n} = (\beta\boldsymbol{\nabla}u^\star)_{\mathrm{i}}\cdot\boldsymbol{n} \quad (\text{on } \Gamma^\star), \tag{4}$$

where subscripts 'm' and 'i' refer to limiting values on $\Gamma^\star$ of quantities in the matrix $\Omega^\star$ and the inclusion $B^\star$, respectively, and β is the conductivity contrast, i.e

$$\beta = k^\star/k. \tag{5}$$

In addition, the *free field* u is defined as the solution to the boundary-value problem

$$\mathrm{div}(k\boldsymbol{\nabla}u)=0 \ \ (\text{in } \Omega), \qquad p=p^{\mathrm{D}} \ \ (\text{on } S_{\mathrm{N}}), \qquad u=u^{\mathrm{D}} \ \ (\text{on } S_{\mathrm{D}}) \tag{6}$$

(with $p=k\boldsymbol{\nabla}u\cdot\boldsymbol{n}$), i.e. is the potential arising in Ω for the same boundary data $p^{\mathrm{D}}, u^{\mathrm{D}}$ in the absence of any trial inclusion.

The following reciprocity identity is now provided for later convenience.

Lemma 1. *Let $(u^\star, u^\star)$ denote a solution to field equations (2) and transmission conditions (4), and let w be any trial field verifying $k\Delta w + b = 0$ in Ω (with b denoting a known source distribution) and continuous, together with its normal flux $k\boldsymbol{\nabla}w\cdot\boldsymbol{n}$, across $\Gamma^\star$. Let β be defined by (5). The following reciprocity identity holds true:*

$$\int_S \big[p[w]u^\star - p^\star w\big]\, d\Gamma + \int_{\Omega^\star} bu^\star\, dV + \int_{B^\star} bu^\star\, dV - (1-\beta)\int_{B^\star} k\boldsymbol{\nabla}u^\star\cdot\boldsymbol{\nabla}w\, dV = 0 \tag{7}$$

Proof. Identity (7) is obtained by means of the third Green's formula

$$\int_{\mathcal{O}} \big[w\Delta u - u\Delta w\big]\, \mathrm{d}V + \int_{\partial\mathcal{O}} \big[(\boldsymbol{\nabla}w\cdot\boldsymbol{n})u - (\boldsymbol{\nabla}u\cdot\boldsymbol{n})w\big]\, \mathrm{d}\Gamma = 0, \tag{8}$$

as follows: (i) write (8) for $\mathcal{O}=\Omega^\star$ and multiply the resulting identity by k; (ii) write (8) for $\mathcal{O}=B^\star$ and multiply the resulting identity by βk; (iii) add the two resulting identities and invoke transmission conditions (4), together with continuity of w and its normal flux, across $\Gamma^\star$, and (iv) use the identity

$$k\int_{\Gamma^\star} (\boldsymbol{\nabla}w\cdot\boldsymbol{n})u\, \mathrm{d}\Gamma = \int_{B^\star} \big[bu - k\boldsymbol{\nabla}u^\star\cdot\boldsymbol{\nabla}w\big]\, \mathrm{d}V,$$

which stems from the divergence theorem (with $\boldsymbol{n}$ denoting here the *inward* unit normal to $\Gamma^\star$). □

2.2 Cost functions

Generic cost functions having the format

$$\mathcal{J}(B^\star) = \int_{S_\mathrm{N}} \varphi_\mathrm{N}(u^\star, \boldsymbol{\xi})\, \mathrm{d}\Gamma + \int_{S_\mathrm{D}} \varphi_\mathrm{D}(p^\star, \boldsymbol{\xi})\, \mathrm{d}\Gamma \tag{9}$$

are considered, where functions φ_N and φ_D are C^2 in their first argument.

For instance, the potential energy $\mathcal{E}(B^\star)$ associated with the solution $(u^\star, u^\star)$ to equations (2) to (4) can be set in the format (9) with

$$\varphi_\mathrm{N}(p^\star, \boldsymbol{\xi}) = -\frac{1}{2} p^\mathrm{D}(\boldsymbol{\xi}) u^\star(\boldsymbol{\xi}), \quad \varphi_\mathrm{D}(p^\star, \boldsymbol{\xi}) = \frac{1}{2} p^\star(\boldsymbol{\xi}) u^\mathrm{D}(\boldsymbol{\xi}) \tag{10}$$

Alternatively, considering the problem of identifying an unknown penetrable inclusion B^true from supplementary data consisting of measured values u^obs of the potential and p^obs of the flux, collected respectively on S_N and S_D (or subsets thereof), the misfit between observations $u^\mathrm{obs}, p^\mathrm{obs}$ and their predictions $u^\star, p^\star$ for a trial inclusion $B^\star$ may also be expressed through a cost function of format (9). For instance, the output least-squares cost function $\mathcal{J}_\mathrm{LS}(B^\star)$ corresponds to

$$\varphi_\mathrm{N}(u^\star, \boldsymbol{\xi}) = \frac{1}{2} \big| u^\star(\boldsymbol{\xi}) - u^\mathrm{obs}(\boldsymbol{\xi}) \big|^2, \quad \varphi_\mathrm{D}(p^\star, \boldsymbol{\xi}) = \frac{1}{2} \big| p^\star(\boldsymbol{\xi}) - p^\mathrm{obs}(\boldsymbol{\xi}) \big|^2. \tag{11}$$

Suitably modified definitions of φ_D and φ_N easily allow to accommodate data available on subsets of S_D or S_N.

In what follows, attention will focus on the case of trial inclusions of small size ε and given location, shape and conductivity contrast. The main objectives of this article are (i) to establish an expansion of cost functions of format (9) with respect to ε, whose coefficients depend on the inclusion location $\boldsymbol{a}$, and (ii) to formulate a computationally fast approximate global search method for inclusion identification exploiting such expansions for misfit functionals.

3 ADJOINT SOLUTION APPROACH FOR EXPANSION OF COST FUNCTION

Let $B_\varepsilon(\boldsymbol{a}) = \boldsymbol{a} + \varepsilon\mathscr{B}$, where $\mathscr{B} \subset \mathbb{R}^2$ is a fixed bounded open set with area $|\mathscr{B}|$ and centered at the origin, define the region of space occupied by a penetrable inclusion of (small) size $\varepsilon > 0$, centered at a specified location $\boldsymbol{a} \in \Omega$. The inclusion shape is hence specified through the choice of normalized domain $\mathscr{B}$ (e.g. $\mathscr{B}$ is the unit disk for a circular small inclusion). The region surrounding the small inclusion is then $\Omega_\varepsilon(\boldsymbol{a}) = \Omega \setminus (B_\varepsilon(\boldsymbol{a}) \cup \Gamma_\varepsilon(\boldsymbol{a}))$.

One is here concerned with small-inclusion approximations of cost functions (9). Accordingly, let $u_\varepsilon(\cdot; \boldsymbol{a})$ denote the solution to equations (2) to (4) with $B^\star = B_\varepsilon(\boldsymbol{a})$, and define $J(\varepsilon; \boldsymbol{a})$ by

$$J(\varepsilon; \boldsymbol{a}) = \mathcal{J}\big(\, B_\varepsilon(\boldsymbol{a}) \,\big) = \int_{S_\mathrm{N}} \varphi_\mathrm{N}(u_\varepsilon, \boldsymbol{\xi})\, \mathrm{d}\Gamma + \int_{S_\mathrm{D}} \varphi_\mathrm{D}(p_\varepsilon, \boldsymbol{\xi})\, \mathrm{d}\Gamma, \tag{12}$$

with $p_\varepsilon \equiv \boldsymbol{\nabla} u_\varepsilon . \boldsymbol{n}$. For notational convenience, explicit references to $\boldsymbol{a}$ will often be omitted in the sequel, e.g. by writing $J(\varepsilon)$ or $u_\varepsilon(\boldsymbol{\xi})$ instead of $J(\varepsilon; \boldsymbol{a})$ or $u_\varepsilon(\boldsymbol{\xi}; \boldsymbol{a})$.

3.1 Expansion of misfit function using adjoint solution

Let v_ε denote the perturbation caused to the potential by a small inclusion nucleating at $\boldsymbol{a}$, i.e.:

$$v_\varepsilon = u_\varepsilon - u \qquad (\text{in } \Omega_\varepsilon \cup B_\varepsilon). \tag{13}$$

It is useful to note that v_ε verifies homogeneous boundary conditions:

$$q_\varepsilon = 0 \ \ (\text{on } S_{\text{N}}), \qquad v_\varepsilon = 0 \ \ (\text{on } S_{\text{D}}) \tag{14}$$

where $q_\varepsilon = k(\boldsymbol{\nabla} v_\varepsilon . \boldsymbol{n})$ is the perturbation of the boundary flux.

Cost functions with quadratic dependence on (u, p) are often considered in applications (e.g. for identification purposes). With this in mind, a polynomial approximation of $J(\varepsilon)$ is sought by exploiting an expansion of (12) to second order in $(v_\varepsilon, q_\varepsilon)$, i.e.:

$$\begin{aligned} J(\varepsilon) = J(0) &+ \int_{S_{\text{N}}} \varphi_{\text{N},u}\ v_\varepsilon \ \text{d}\Gamma + \int_{S_{\text{D}}} \varphi_{\text{D},p}\ q_\varepsilon \ \text{d}\Gamma \\ &+ \frac{1}{2}\int_{S_{\text{N}}} \varphi_{\text{N},uu}\ (v_\varepsilon)^2 \ \text{d}\Gamma + \frac{1}{2}\int_{S_{\text{D}}} \varphi_{\text{D},pp}\ (q_\varepsilon)^2 \ \text{d}\Gamma + o\big(\, |v_\varepsilon|^2_{L^2(S_{\text{N}})}\,,\, |q_\varepsilon|^2_{L^2(S_{\text{D}})}\,\big), \end{aligned} \tag{15}$$

having set

$$\varphi_{\text{N},u} = \frac{\partial \varphi_{\text{N}}}{\partial u_\varepsilon}\Big|_{u_\varepsilon = u}, \quad \varphi_{\text{D},p} = \frac{\partial \varphi_{\text{D}}}{\partial p_\varepsilon}\Big|_{p_\varepsilon = p}, \quad \varphi_{\text{N},uu} = \frac{\partial^2 \varphi_{\text{N}}}{\partial u_\varepsilon^2}\Big|_{u_\varepsilon = u}, \quad \varphi_{\text{D},pp} = \frac{\partial^2 \varphi_{\text{D}}}{\partial p_\varepsilon^2}\Big|_{p_\varepsilon = p} \tag{16}$$

In particular, the above quantities are given by

$$\varphi_{\text{D},p} = \frac{1}{2}u^{\text{D}}, \quad \varphi_{\text{N},u} = -\frac{1}{2}p^{\text{D}}, \quad \varphi_{\text{D},pp} = 0, \quad \varphi_{\text{N},uu} = 0 \tag{17}$$

for $\varphi_{\text{N}}, \varphi_{\text{D}}$ defined by (10), and

$$\varphi_{\text{N},u} = u - u^{\text{obs}}, \quad \varphi_{\text{D},p} = p - p^{\text{obs}}, \quad \varphi_{\text{N},uu} = 1, \quad \varphi_{\text{D},pp} = 1 \tag{18}$$

for $\varphi_{\text{N}}, \varphi_{\text{D}}$ defined by (11). Expansion (15) is exact, i.e. has a zero remainder, for the potential energy defined by (10) and the least-squares misfit functions (11).

Lemma 2 (reformulation of cost function expansion using an adjoint solution)**.** *Let the* adjoint field $\hat{u}$ *be defined as the solution of the adjoint problem*

$$k\Delta\hat{u} = 0 \ \ (\textit{in } \Omega)\ , \quad \hat{p} = \varphi_{N,u} \ \ (\textit{on } S_N)\ , \quad \hat{u} = -\varphi_{D,p} \ \ (\textit{on } S_D). \tag{19}$$

(with $\hat{p} = k\boldsymbol{\nabla}\hat{u}\cdot\boldsymbol{n}$). Expansion (15) then admits the alternative form

$$\begin{aligned} J(\varepsilon) = J(0) &+ (1-\beta)\int_{B_\varepsilon} k\boldsymbol{\nabla} u_\varepsilon \cdot \boldsymbol{\nabla}\hat{u}\ dV \\ &+ \frac{1}{2}\int_{S_N} \varphi_{N,uu}\ (v_\varepsilon)^2\ d\Gamma + \frac{1}{2}\int_{S_D} \varphi_{D,pp}\ (q_\varepsilon)^2\ d\Gamma + o(|v_\varepsilon|^2_{L^2(S_N)}\,,\, |q_\varepsilon|^2_{L^2(S_D)}), \end{aligned} \tag{20}$$

Proof. Invoking reciprocity identity (7) with $w = \hat{u},\ b = 0$ and boundary conditions (14) and (19b,c), one obtains identity

$$\int_{S_{\text{N}}} \varphi_{\text{N},u}\ v_\varepsilon \ \text{d}\Gamma + \int_{S_{\text{D}}} \varphi_{\text{D},p}\ q_\varepsilon \ \text{d}\Gamma = (1-\beta)\int_{B_\varepsilon} k\boldsymbol{\nabla} u_\varepsilon \cdot \boldsymbol{\nabla}\hat{u}\ \text{d}V$$

which, inserted into expansion (15), yields the desired reformulation (20). □

3.2 Summary of previous results on topological sensitivity

In previous studies [14, 20], the leading contribution to $J(\varepsilon)$ has been found, on the basis of identity (20) truncated to first order in $(v_\varepsilon, q_\varepsilon)$ (i.e. without the last two integrals), to be given by

$$J(\varepsilon) = J(0) + \varepsilon^2 \mathcal{T}_2(\boldsymbol{a}; \mathscr{B}, \beta) + o(\varepsilon^3) \tag{21}$$

in terms of the *topological derivative* $\mathcal{T}_2(\boldsymbol{a}; \mathscr{B}, \beta)$, given in the present context of 2-D potential problems by

$$\mathcal{T}_2(\boldsymbol{a}; \mathscr{B}, \beta) = \boldsymbol{\nabla}\hat{u}(\boldsymbol{a}) \cdot \boldsymbol{\mathcal{A}}_{11}(\mathscr{B}, \beta) \cdot \boldsymbol{\nabla} u(\boldsymbol{a}) \tag{22}$$

where the second-order 'polarization tensor' $\boldsymbol{\mathcal{A}}_{11}(\mathscr{B}, \beta)$ has been established for any inclusion shape $\mathscr{B}$ and conductivity contrast β in [20]. For the simplest case of a circular inclusion, where $\mathscr{B}$ is the unit disk, one has the explicit expression

$$\boldsymbol{\mathcal{A}}_{11} = 2\pi \frac{(1-\beta)}{1+\beta} \boldsymbol{I}. \tag{23}$$

(where $\boldsymbol{I}$ is the seccond-order identity tensor). Moreover, the leading asymptotic behaviour of the perturbed field is characterized by

$$v_\varepsilon(\boldsymbol{x}) = \varepsilon^2 W(\boldsymbol{x}) + o(\varepsilon^2), \qquad q_\varepsilon(\boldsymbol{x}) = \varepsilon^2 \boldsymbol{\nabla} Q(\boldsymbol{x}) + o(\varepsilon^2) \qquad (\boldsymbol{x} \in S) \tag{24}$$

(having set $Q(\boldsymbol{x}) = \boldsymbol{\nabla} W(\boldsymbol{x}) \cdot \boldsymbol{n}(\boldsymbol{x})$) on the external boundary, and by

$$v_\varepsilon(\boldsymbol{x}) = \varepsilon V_1\big((\boldsymbol{x} - \boldsymbol{a})/\varepsilon\big) + o(\varepsilon) \qquad (\boldsymbol{x} \in B_\varepsilon) \tag{25}$$

inside $\mathscr{B}$, where the functions W and V_1 are known and depend on $\mathscr{B}$ and β (see Eqs. (57) and (48a)).

3.3 Derivation of expansion of $J(\varepsilon)$: methodology and notation

To capture the leading contribution as $\varepsilon \to 0$ of the quadratic terms v_ε^2 and q_ε^2, an expansion of $J(\varepsilon)$ must, in view of (20) and (24), be performed to order $O(\varepsilon^4)$ at least. As (20) involves integrals over the vanishing support B_ε, the position vector $\bar{\boldsymbol{\xi}} \in B_\varepsilon$ is scaled for this purpose according to:

$$\boldsymbol{\xi} = \boldsymbol{a} + \varepsilon \bar{\boldsymbol{\xi}} \qquad (\boldsymbol{\xi} \in B_\varepsilon,\, \bar{\boldsymbol{\xi}} \in \mathscr{B}) \tag{26}$$

In particular, this mapping transforms integrals over B_ε into integrals over $\mathscr{B}$, and rescales the domain differential element according to

$$\mathrm{d}V_\xi = \varepsilon^2 \, \mathrm{d}\bar{V}_{\bar{\xi}} \quad (\boldsymbol{\xi} \in B_\varepsilon,\, \bar{\boldsymbol{\xi}} \in \mathscr{B}) \tag{27}$$

Without loss of generality, $\boldsymbol{a}$ can be chosen as the center of B_ε, i.e. such that

$$\int_{\mathscr{B}} \bar{\boldsymbol{\xi}} \, \mathrm{d}\bar{V}_{\bar{\xi}} = \boldsymbol{0}. \tag{28}$$

In view of (27), establishing the sought $O(\varepsilon^4)$ expansion of $J(\varepsilon)$ requires a $O(\varepsilon^2)$ expansion of $\boldsymbol{\nabla} u_\varepsilon$ in B_ε. Taking the previously known behavior (25) into account, an asymptotic expression for small ε of the total field u_ε inside the inclusion is sought in the form

$$u_\varepsilon(\boldsymbol{\xi}) = u(\boldsymbol{\xi}) + \varepsilon V_1(\bar{\boldsymbol{\xi}}) + \varepsilon^2 V_2(\bar{\boldsymbol{\xi}}) + \frac{1}{2}\varepsilon^3 V_3(\bar{\boldsymbol{\xi}}) + o(\varepsilon^3) \qquad (\boldsymbol{\xi} \in B_\varepsilon, \bar{\boldsymbol{\xi}} \in \mathscr{B}) \tag{29}$$

in terms of unknown functions V_1, V_2, V_3 defined in $\mathscr{B}$. The determination of V_1, V_2, V_3, which constitutes the main step towards establishing an explicit expression for the expansion of $J(\varepsilon)$, is based on expanding about $\varepsilon \to 0$ an integral equation formulation for u_ε. This task is addressed in the next section.

4 EXPANSION OF FIELD INSIDE THE INCLUSION

4.1 Integral equation formulation of the forward problem

Let the Green's function $\mathcal{G}(\boldsymbol{x}, \boldsymbol{\xi})$ associated with the domain Ω and partition $S = S_{\mathrm{N}} \cup S_{\mathrm{D}}$ of the external boundary be defined by

$$\begin{aligned} k\Delta_\xi \mathcal{G}(\boldsymbol{x}, \boldsymbol{\xi}) + \delta(\boldsymbol{\xi} - \boldsymbol{x}) = 0 \ \ (\boldsymbol{\xi} \in \Omega) \\ \mathcal{H}(\boldsymbol{x}, \boldsymbol{\xi}) = 0 \ \ (\boldsymbol{\xi} \in S_{\mathrm{N}}), \\ \mathcal{G}(\boldsymbol{x}, \boldsymbol{\xi}) = 0 \ \ (\boldsymbol{\xi} \in S_{\mathrm{D}}) \end{aligned} \tag{30}$$

(with $\mathcal{H}(\boldsymbol{x}, \boldsymbol{\xi}) = k\boldsymbol{\nabla}_\xi \mathcal{G}(\boldsymbol{x}, \boldsymbol{\xi}) \cdot \boldsymbol{n}(\boldsymbol{\xi})$). On using $w(\boldsymbol{\xi}) = \mathcal{G}(\boldsymbol{x}, \boldsymbol{\xi})$, i.e. $b(\boldsymbol{\xi}) = \delta(\boldsymbol{\xi} - \boldsymbol{x})$ in the reciprocity identity (7) and inserting boundary conditions (3), one obtains the following governing integral equation for the field u_ε inside the inclusion B_ε, which solves the forward problem (2)–(4) with $B^\star = B_\varepsilon$:

$$u_\varepsilon(\boldsymbol{x}) - \int_{B_\varepsilon} (1-\beta) k \boldsymbol{\nabla} u_\varepsilon(\boldsymbol{\xi}) \cdot \boldsymbol{\nabla}_\xi \mathcal{G}(\boldsymbol{x}, \boldsymbol{\xi}) \, \mathrm{d}V_\xi = u(\boldsymbol{x}) \qquad (\boldsymbol{x} \in B_\varepsilon), \tag{31}$$

where u, the free field defined by (6), is here explicitly given by

$$u(\boldsymbol{x}) = \int_{S_{\mathrm{N}}} \mathcal{G}(\boldsymbol{x}, \boldsymbol{\xi}) \, p^{\mathrm{D}}(\boldsymbol{\xi}) \, \mathrm{d}\Gamma_\xi - \int_{S_{\mathrm{D}}} \mathcal{H}(\boldsymbol{x}, \boldsymbol{\xi}) \, u^{\mathrm{D}}(\boldsymbol{\xi}) \, \mathrm{d}\Gamma_\xi \qquad (\boldsymbol{x} \in \Omega). \tag{32}$$

Similarly, the adjoint field defined by (19) admits the explicit integral representation formula

$$\hat{u}(\boldsymbol{x}) = \int_{S_{\mathrm{N}}} \mathcal{G}(\boldsymbol{x}, \boldsymbol{\xi}) \, \varphi_{\mathrm{N},u}(\boldsymbol{\xi}) \, \mathrm{d}\Gamma_\xi + \int_{S_{\mathrm{D}}} \mathcal{H}(\boldsymbol{x}, \boldsymbol{\xi}) \, \varphi_{\mathrm{D},p}(\boldsymbol{\xi}) \, \mathrm{d}\Gamma_\xi \qquad (\boldsymbol{x} \in \Omega). \tag{33}$$

Note that equation (31) is also valid for a non-uniform conductivity contrast β, a feature not exploited in this work. Moreover, the field outside the inclusion is given by the representation formula

$$u_\varepsilon(\boldsymbol{x}) = (1-\beta) k \int_{B_\varepsilon} \boldsymbol{\nabla} u_\varepsilon(\boldsymbol{\xi}) \cdot \boldsymbol{\nabla}_\xi \mathcal{G}(\boldsymbol{x}, \boldsymbol{\xi}) \, \mathrm{d}V_\xi + u(\boldsymbol{x}) \qquad (\boldsymbol{x} \in \Omega \setminus B_\varepsilon), \tag{34}$$

Under the assumption of a constant conductivity inside the inclusion, a governing boundary integral equation formulation that is equivalent to (31) reads

$$\frac{1+\beta}{2} u_\varepsilon(\boldsymbol{x}) - (1-\beta) k \int_{\Gamma_\varepsilon} \mathcal{H}(\boldsymbol{\xi}, \boldsymbol{x}) u_\varepsilon(\boldsymbol{\xi}) \, \mathrm{d}\Gamma_\xi = u(\boldsymbol{x}) \qquad (\boldsymbol{x} \in \Gamma_\varepsilon). \tag{35}$$

4.2 Small-inclusion expansion of the integral equation

To study the asymptotic behaviour of integral equation (31) as $\varepsilon \to 0$, it is useful to introduce further scaled geometric quantities:

$$\boldsymbol{x} = \varepsilon \bar{\boldsymbol{x}}\ , \quad \boldsymbol{r} = \varepsilon \bar{\boldsymbol{r}}\ , \quad r = \varepsilon \bar{r} \qquad (\boldsymbol{x}, \boldsymbol{\xi} \in B_\varepsilon;\ \bar{\boldsymbol{x}}, \bar{\boldsymbol{\xi}} \in \mathscr{B}) \tag{36}$$

in addition to definition (26) of $\bar{\boldsymbol{\xi}}$, and to split the Green's function according to:

$$\mathcal{G}(\boldsymbol{x}, \boldsymbol{\xi}) = G(\boldsymbol{x}, \boldsymbol{\xi}) + G_{\mathrm{C}}(\boldsymbol{x}, \boldsymbol{\xi}), \tag{37}$$

where G is the well-known fundamental solution for the 2-D full space, given by

$$G(\boldsymbol{x}, \boldsymbol{\xi}) = -\frac{1}{2k\pi}\mathrm{Log} r, \qquad \boldsymbol{\nabla}_\xi G(\boldsymbol{x}, \boldsymbol{\xi}) = -\frac{1}{2k\pi r^2}\boldsymbol{r} \tag{38}$$

with $\boldsymbol{r} = \boldsymbol{\xi} - \boldsymbol{x}$ and $r = |\boldsymbol{\xi} - \boldsymbol{x}| = |\boldsymbol{r}|$, and the complementary part G_{C} is smooth at $\boldsymbol{\xi} = \boldsymbol{x}$.

Lemma 3. *Using the ansatz (29) for the field u_ε inside B_ε (with functions V_1, V_2, V_3 to be determined later), integral equation (31) has the following $O(\varepsilon^3)$ expansion about $\varepsilon = 0$:*

$$\varepsilon\Big\{\big[(\mathcal{I} - \bar{\mathcal{L}})V_1\big](\bar{\boldsymbol{x}}) - \mathcal{F}_1(\bar{\boldsymbol{x}})\Big\} + \varepsilon^2\Big\{\big[(\mathcal{I} - \bar{\mathcal{L}})V_2\big](\bar{\boldsymbol{x}}) - \mathcal{F}_2(\bar{\boldsymbol{x}})\Big\} + \frac{1}{2}\varepsilon^3\Big\{\big[(\mathcal{I} - \bar{\mathcal{L}})V_3\big](\bar{\boldsymbol{x}}) - \mathcal{F}_3(\bar{\boldsymbol{x}})\Big\} + o(\varepsilon^3) = 0, \tag{39}$$

where $\mathcal{I}$ denotes the identity, the integral operator $\bar{\mathcal{L}}$ is defined for scalar, vector or tensor density functions $f(\bar{\boldsymbol{\xi}}),\ \bar{\boldsymbol{\xi}} \in \mathscr{B}$ by

$$\big[\bar{\mathcal{L}} f\big](\bar{\boldsymbol{x}}) = (1-\beta)k \int_{\mathscr{B}} \bar{\boldsymbol{\nabla}} f(\bar{\boldsymbol{\xi}}) \cdot \bar{\boldsymbol{\nabla}} G(\bar{\boldsymbol{x}}, \bar{\boldsymbol{\xi}})\ d\bar{V}_{\bar{\xi}} \qquad (\bar{\boldsymbol{x}} \in \mathscr{B}), \tag{40}$$

(with $\bar{\boldsymbol{\nabla}} \equiv \boldsymbol{\nabla}_{\bar{\xi}}$ denoting the gradient with respect to normalized coordinates) and $\mathcal{F}_1(\bar{\boldsymbol{x}}),\ \mathcal{F}_2(\bar{\boldsymbol{x}}),\ \mathcal{F}_3(\bar{\boldsymbol{x}})$ are given by

$$\mathcal{F}_1(\bar{\boldsymbol{x}}) = \boldsymbol{\nabla} u(\boldsymbol{a}) \cdot \big[\bar{\mathcal{L}}\bar{\boldsymbol{\xi}}\big](\bar{\boldsymbol{x}}) \tag{41a}$$

$$\mathcal{F}_2(\bar{\boldsymbol{x}}) = \frac{1}{2}\boldsymbol{\nabla}^2 u(\boldsymbol{a}) : \big[\bar{\mathcal{L}}(\bar{\boldsymbol{\xi}} \otimes \bar{\boldsymbol{\xi}})\big](\bar{\boldsymbol{x}}) + F(\boldsymbol{a}) \tag{41b}$$

$$\mathcal{F}_3(\bar{\boldsymbol{x}}) = \frac{1}{3}\boldsymbol{\nabla}^3 u(\boldsymbol{a}) \vdots \big[\bar{\mathcal{L}}(\bar{\boldsymbol{\xi}} \otimes \bar{\boldsymbol{\xi}} \otimes \bar{\boldsymbol{\xi}})\big](\bar{\boldsymbol{x}}) + 2\bar{\boldsymbol{x}} \cdot \boldsymbol{\nabla} F(\boldsymbol{a}) + 2G(\boldsymbol{a}) \tag{41c}$$

where $\boldsymbol{\nabla}^k u(\boldsymbol{a})$ denotes the k-th order gradient of u evaluated at $\boldsymbol{\xi} = \boldsymbol{a}$, and having set

$$F(\boldsymbol{z}) = (1-\beta)k\Big(|\mathscr{B}|\,\boldsymbol{\nabla} u(\boldsymbol{a}) + \int_{\mathscr{B}} \bar{\boldsymbol{\nabla}} V_1(\bar{\boldsymbol{\xi}})\ d\bar{V}_{\bar{\xi}}\Big) \cdot \boldsymbol{\nabla} G_C(\boldsymbol{z}, \boldsymbol{a}) \tag{42a}$$

$$G(\boldsymbol{z}) = (1-\beta)k\Big\{\Big(\int_{\mathscr{B}} \bar{\boldsymbol{\nabla}} V_1(\bar{\boldsymbol{\xi}}) \otimes \bar{\boldsymbol{\xi}}\ d\bar{V}_{\bar{\xi}}\Big) : \boldsymbol{\nabla}^2 G_C(\boldsymbol{z}, \boldsymbol{a}) + \Big(\int_{\mathscr{B}} \bar{\boldsymbol{\nabla}} V_2(\bar{\boldsymbol{\xi}})\ d\bar{V}_{\bar{\xi}}\Big) \cdot \boldsymbol{\nabla} G_C(\boldsymbol{z}, \boldsymbol{a})\Big\} \tag{42b}$$

Proof. The proof rests on splitting the Green's function according to (37) in integral equation (31) and using the following expansion of $\boldsymbol{\nabla} u_\varepsilon$, obtained from (29)

$$\boldsymbol{\nabla} u_\varepsilon(\boldsymbol{\xi}) = \boldsymbol{\nabla} u(\boldsymbol{a}) + \bar{\boldsymbol{\nabla}} V_1(\bar{\boldsymbol{\xi}}) + \varepsilon\big[\,\boldsymbol{\nabla}^2 u(\boldsymbol{a}) \cdot \bar{\boldsymbol{\xi}} + \bar{\boldsymbol{\nabla}} V_2(\bar{\boldsymbol{\xi}})\,\big] + \frac{1}{2}\varepsilon^2\big[\,\boldsymbol{\nabla}^3 u(\boldsymbol{a}) : (\bar{\boldsymbol{\xi}} \otimes \bar{\boldsymbol{\xi}}) + \bar{\boldsymbol{\nabla}} V_3(\bar{\boldsymbol{\xi}})\,\big] + o(\varepsilon^2). \tag{43}$$

First, noting that upon scaling the position vector according to (36) the singular full-space fundamental solution verifies

$$\boldsymbol{\nabla}_{\xi} G(\boldsymbol{x},\boldsymbol{\xi}) = -\frac{1}{\varepsilon}\frac{1}{2k\pi\bar{r}^2}\bar{\boldsymbol{r}} = \frac{1}{\varepsilon}\boldsymbol{\nabla} G(\bar{\boldsymbol{x}},\bar{\boldsymbol{\xi}}), \tag{44}$$

one finds

$$\begin{aligned}(1-\beta)\int_{B_\varepsilon} k\boldsymbol{\nabla} u_\varepsilon(\boldsymbol{\xi})\cdot\boldsymbol{\nabla}_{\xi} G(\boldsymbol{x},\boldsymbol{\xi})\,\mathrm{d}V_\xi = \varepsilon\Big(\big[\bar{\mathcal{L}}V_1\big] + \boldsymbol{\nabla} u(\boldsymbol{a})\cdot\big[\bar{\mathcal{L}}\bar{\boldsymbol{\xi}}\big]\Big)(\bar{\boldsymbol{x}}) \\ + \varepsilon^2\Big(\big[\bar{\mathcal{L}}V_2\big] + \frac{1}{2}\boldsymbol{\nabla}^2 u(\boldsymbol{a}) : \big[\bar{\mathcal{L}}(\bar{\boldsymbol{\xi}}\otimes\bar{\boldsymbol{\xi}})\big]\Big)(\bar{\boldsymbol{x}}) \\ + \frac{\varepsilon^3}{2}\Big(\big[\bar{\mathcal{L}}V_3\big] + \frac{1}{3}\boldsymbol{\nabla}^3 u(\boldsymbol{a}) : \big[\bar{\mathcal{L}}(\bar{\boldsymbol{\xi}}\otimes\bar{\boldsymbol{\xi}}\otimes\bar{\boldsymbol{\xi}})\big]\Big)(\bar{\boldsymbol{x}})\end{aligned} \tag{45}$$

with the help of differential element scaling (27) and expansion (43), and invoking definition (40) of integral operator $\bar{\mathcal{L}}$.

Second, as the complementary kernel $G_{\mathrm{C}}(\boldsymbol{x},\boldsymbol{\xi})$ is smooth when $\boldsymbol{x}=\boldsymbol{\xi}$, the following Taylor expansion holds for any $\bar{\boldsymbol{x}},\bar{\boldsymbol{\xi}}\in\mathscr{B}$:

$$\boldsymbol{\nabla}_{\xi} G_{\mathrm{C}}(\boldsymbol{x},\boldsymbol{\xi}) = \boldsymbol{\nabla} G_{\mathrm{C}}(\boldsymbol{a},\boldsymbol{a}) + \varepsilon\big[(\bar{\boldsymbol{x}}\cdot\boldsymbol{\nabla}_x + \bar{\boldsymbol{\xi}}\cdot\boldsymbol{\nabla}_{\xi})\boldsymbol{\nabla}_{\xi} G_{\mathrm{C}}\big](\boldsymbol{a},\boldsymbol{a}) + o(\varepsilon). \tag{46}$$

On performing a derivation which consists of (i) expanding to order $O(\varepsilon)$ the inner product of expansions (29) and (46), (ii) integrating the result over B_ε and multiplying the result by $(1-\beta)k$, (iii) invoking scaling (27), (iv) using integral identity (28), and (v) exploiting definitions (42a,b), one finds

$$(1-\beta)\int_{B_\varepsilon} k\boldsymbol{\nabla} u_\varepsilon(\boldsymbol{\xi})\cdot\boldsymbol{\nabla}_{\xi} G_{\mathrm{C}}(\boldsymbol{x},\boldsymbol{\xi})\,\mathrm{d}V_\xi = \varepsilon^2 F(\boldsymbol{a}) + \varepsilon^3\big(\boldsymbol{\nabla} F(\boldsymbol{a}) + G(\boldsymbol{a})\big). \tag{47}$$

Lemma 3 finally follows from substituting expansions (29), (45) and (47) into integral equation (31) and reordering contributions according to powers of ε. □

4.3 Expansion of potential inside the inclusion

Lemma 4. *The $O(\varepsilon^3)$ expansion (29) of u_ε is given by*

$$V_1(\bar{\boldsymbol{\xi}}) = \boldsymbol{\mathcal{U}}_1(\bar{\boldsymbol{\xi}})\cdot\boldsymbol{\nabla} u(\boldsymbol{a}) \tag{48a}$$

$$V_2(\bar{\boldsymbol{\xi}}) = \boldsymbol{\mathcal{U}}_2(\bar{\boldsymbol{\xi}}) : \boldsymbol{\nabla}^2 u(\boldsymbol{a}) + F(\boldsymbol{a}) \tag{48b}$$

$$V_3(\bar{\boldsymbol{\xi}}) = \boldsymbol{\mathcal{U}}_3(\bar{\boldsymbol{\xi}}) \vdots \boldsymbol{\nabla}^3 u(\boldsymbol{a}) + 2\big[\bar{\boldsymbol{\xi}} + \boldsymbol{\mathcal{U}}_1(\bar{\boldsymbol{\xi}})\big]\cdot\boldsymbol{\nabla} F(\boldsymbol{a}) + 2G(\boldsymbol{a}) \tag{48c}$$

where the vector function $\boldsymbol{\mathcal{U}}_1$, the second-order tensor function $\boldsymbol{\mathcal{U}}_2$ and the third-order tensor function $\boldsymbol{\mathcal{U}}_3$ do not depend on $\boldsymbol{a}$ and solve the integral equations

$$\big[(\mathcal{I}-\bar{\mathcal{L}})\boldsymbol{\mathcal{U}}_1\big](\bar{\boldsymbol{x}}) = \big[\bar{\mathcal{L}}\bar{\boldsymbol{\xi}}\big](\bar{\boldsymbol{x}}) \tag{49a}$$

$$\big[(\mathcal{I}-\bar{\mathcal{L}})\boldsymbol{\mathcal{U}}_2\big](\bar{\boldsymbol{x}}) = \frac{1}{2}\big[\bar{\mathcal{L}}(\bar{\boldsymbol{\xi}}\otimes\bar{\boldsymbol{\xi}})\big](\bar{\boldsymbol{x}}) \tag{49b}$$

$$\big[(\mathcal{I}-\bar{\mathcal{L}})\boldsymbol{\mathcal{U}}_3\big](\bar{\boldsymbol{x}}) = \frac{1}{3}\big[\bar{\mathcal{L}}(\bar{\boldsymbol{\xi}}\otimes\bar{\boldsymbol{\xi}}\otimes\bar{\boldsymbol{\xi}})\big](\bar{\boldsymbol{x}}) \tag{49c}$$

(with $\bar{\mathcal{L}}$ defined by 40). Moreover, the scalar functions $F(\boldsymbol{x}), G(\boldsymbol{x})$ defined by (42a,b) are given for any $\boldsymbol{x} \in \Omega$ by

$$F(\boldsymbol{x}) = \boldsymbol{\nabla} u(\boldsymbol{a}) \cdot \boldsymbol{\mathcal{A}}_{11} \cdot \boldsymbol{\nabla} G_C(\boldsymbol{x}, \boldsymbol{a}) \tag{50a}$$

$$G(\boldsymbol{x}) = \boldsymbol{\nabla} u(\boldsymbol{a}) \cdot \boldsymbol{\mathcal{A}}_{12} : \boldsymbol{\nabla}^2 G_C(\boldsymbol{x}, \boldsymbol{a}) + \boldsymbol{\nabla} G_C(\boldsymbol{x}, \boldsymbol{a}) \cdot \boldsymbol{\mathcal{A}}_{12} : \boldsymbol{\nabla}^2 u(\boldsymbol{a}), \tag{50b}$$

with the constant tensors $\boldsymbol{\mathcal{A}}_{11}, \boldsymbol{\mathcal{A}}_{12}$ (respectively of order 2 and 3) defined by

$$\boldsymbol{\mathcal{A}}_{11} = (1-\beta) k \Big(|\mathscr{B}| \, \boldsymbol{I} + \int_{\mathscr{B}} \bar{\boldsymbol{\nabla}} \boldsymbol{\mathcal{U}}_1(\bar{\boldsymbol{\xi}}) \, d\bar{V}_{\bar{\xi}} \Big) \tag{51a}$$

$$\boldsymbol{\mathcal{A}}_{12} = (1-\beta) k \int_{\mathscr{B}} \bar{\boldsymbol{\nabla}} \boldsymbol{\mathcal{U}}_1(\bar{\boldsymbol{\xi}}) \otimes \bar{\boldsymbol{\xi}} \, d\bar{V}_{\bar{\xi}} \tag{51b}$$

Proof. Definitions (41a) and (49a) immediately imply that

$$\mathcal{F}_1(\bar{\boldsymbol{x}}) = \Big[(\mathcal{I} - \bar{\mathcal{L}}) \Big(\boldsymbol{\mathcal{U}}_1(\bar{\boldsymbol{\xi}}) \cdot \boldsymbol{\nabla} u(\boldsymbol{a}) \Big) \Big] (\bar{\boldsymbol{x}})$$

Similarly, on using definitions (41b), (49b) and noting that $1 = \big[(\mathcal{I} - \bar{\mathcal{L}}) 1\big](\bar{\boldsymbol{x}})$, one obtains

$$\mathcal{F}_2(\bar{\boldsymbol{x}}) = \Big[(\mathcal{I} - \bar{\mathcal{L}}) \Big(\boldsymbol{\mathcal{U}}_2(\bar{\boldsymbol{\xi}}) : \boldsymbol{\nabla}^2 u(\boldsymbol{a}) + F(\boldsymbol{a}) \Big) \Big] (\bar{\boldsymbol{x}})$$

Finally, one notes that definition (49a) implies that $\bar{\boldsymbol{x}} = \big[(\mathcal{I} - \bar{\mathcal{L}}) \big(\bar{\boldsymbol{\xi}} + \boldsymbol{\mathcal{U}}_1(\bar{\boldsymbol{\xi}}) \big) \big] (\bar{\boldsymbol{x}})$. Using this identity together with identity $1 = \big[(\mathcal{I} - \bar{\mathcal{L}}) 1\big](\bar{\boldsymbol{x}})$ (again) and definitions (41c) and (49c), one obtains

$$\mathcal{F}_3(\bar{\boldsymbol{x}}) = \Big[(\mathcal{I} - \bar{\mathcal{L}}) \Big(\boldsymbol{\mathcal{U}}_3(\bar{\boldsymbol{\xi}}) \vdots \boldsymbol{\nabla}^3 u(\boldsymbol{a}) + 2 \big(\bar{\boldsymbol{\xi}} + \boldsymbol{\mathcal{U}}_1(\bar{\boldsymbol{\xi}}) \big) \cdot \boldsymbol{\nabla} F(\boldsymbol{a}) + 2 G(\boldsymbol{a}) \Big) \Big] (\bar{\boldsymbol{x}})$$

Representations (48a–c) follow directly from the previous three identities by virtue of the fact that integral operator $\mathcal{I} - \bar{\mathcal{L}}$ is invertible.

Then, definitions (51a,b) and reformulations (50a,b) of $F(\boldsymbol{x}), G(\boldsymbol{x})$ stem directly from substituting representations (48a,b) into (42a,b) and exploiting property (52a) of functions $\boldsymbol{\mathcal{U}}_1, \boldsymbol{\mathcal{U}}_2$, see Lemma 5 next. □

Lemma 5. *Functions $\boldsymbol{\mathcal{U}}_1, \boldsymbol{\mathcal{U}}_2$ defined by lemma 4 are such that*

$$\boldsymbol{\nabla}^2 w(\boldsymbol{a}) : \Big(\int_{\mathscr{B}} \bar{\boldsymbol{\nabla}} \boldsymbol{\mathcal{U}}_2(\bar{\boldsymbol{\xi}}) \, d\bar{V}_{\bar{\xi}} \Big) = \Big(\int_{\mathscr{B}} \bar{\boldsymbol{\nabla}} \boldsymbol{\mathcal{U}}_1(\bar{\boldsymbol{\xi}}) \otimes \bar{\boldsymbol{\xi}} \, d\bar{V}_{\bar{\xi}} \Big) : \boldsymbol{\nabla}^2 w(\boldsymbol{a}) \tag{52a}$$

$$\boldsymbol{\nabla}^3 w(\boldsymbol{a}) \vdots \Big(\int_{\mathscr{B}} \bar{\boldsymbol{\nabla}} \boldsymbol{\mathcal{U}}_3(\bar{\boldsymbol{\xi}}) \, d\bar{V}_{\bar{\xi}} \Big) = \Big(\int_{\mathscr{B}} \bar{\boldsymbol{\nabla}} \boldsymbol{\mathcal{U}}_1(\bar{\boldsymbol{\xi}}) \otimes (\bar{\boldsymbol{\xi}} \otimes \bar{\boldsymbol{\xi}}) \, d\bar{V}_{\bar{\xi}} \Big) \vdots \boldsymbol{\nabla}^3 w(\boldsymbol{a}) \tag{52b}$$

for any sufficiently regular function w.

Proof. As functions $\boldsymbol{\mathcal{U}}_1, \boldsymbol{\mathcal{U}}_2, \boldsymbol{\mathcal{U}}_3$ verify the weak formulation (B.2) with $U^0 = \bar{\boldsymbol{\xi}}$, $U^0 = (\bar{\boldsymbol{\xi}} \otimes \bar{\boldsymbol{\xi}})/2$ and $U^0 = (\bar{\boldsymbol{\xi}} \otimes \bar{\boldsymbol{\xi}} \otimes \bar{\boldsymbol{\xi}})/3$, respectively (see Appendix B), the following identities hold:

$$\mathcal{A}(\boldsymbol{\mathcal{U}}_{1a}, W) = \int_{\mathscr{B}} k^\star W_{,a} \, \mathrm{d}\bar{V}_{\bar{\xi}} \qquad (a = 1, 2) \tag{53a}$$

$$\mathcal{A}(\boldsymbol{\mathcal{U}}_{2ab}, W), = \frac{1}{2} \int_{\mathscr{B}} k^\star (\bar{\xi}_a W_{,b} + W_{,a} \bar{\xi}_b) \, \mathrm{d}\bar{V}_{\bar{\xi}} \qquad (a, b = 1, 2) \tag{53b}$$

$$\mathcal{A}(\boldsymbol{\mathcal{U}}_{3abc}, W), = \frac{1}{3} \int_{\mathscr{B}} k^\star (W_{,a} \bar{\xi}_b \bar{\xi}_c + \bar{\xi}_a W_{,b} \bar{\xi}_c + \bar{\xi}_a \bar{\xi}_b W_{,c}) \, \mathrm{d}\bar{V}_{\bar{\xi}} \qquad (a, b, c = 1, 2), \tag{53c}$$

with $\mathcal{A}(\cdot,\cdot)$ defined by (B.3). Setting $W = \boldsymbol{\mathcal{U}}_{2jk}$ and $a = i$ in (53a), $W = \boldsymbol{\mathcal{U}}_{1i}$ and $(a,b) = (j,k)$ in (53b), subtracting the resulting identities and using the symmetry of bilinear form $a(\cdot,\cdot)$, one obtains

$$\int_{\mathscr{B}} k^\star \boldsymbol{\mathcal{U}}_{2jk,i}\, \mathrm{d}\bar{V}_{\bar{\xi}} = \frac{1}{2}\int_{\mathscr{B}} k^\star(\boldsymbol{\mathcal{U}}_{1i,k}\bar{\xi}_j + \boldsymbol{\mathcal{U}}_{1j,k}\bar{\xi}_i)\, \mathrm{d}\bar{V}_{\bar{\xi}}$$

The desired identity (52a) is then obtained by multiplying the above equation by $w_{,jk}(\bar{\boldsymbol{x}})$ and invoking $w_{,jk} = w_{,kj}$ (Schwarz theorem). Identity (52b) is established in a similar manner by combining (53a) with $W = \boldsymbol{\mathcal{U}}_3$ and (53c) with $W = \boldsymbol{\mathcal{U}}_1$. □

5 TOPOLOGICAL EXPANSION OF COST FUNCTION

Building on the results established thus far, the $O(\varepsilon^4)$ expansion of $J(\varepsilon)$, is now formulated. The most general form of the proposed $O(\varepsilon^4)$ expansion, valid for a small inclusion of arbitrary shape, is given first (Sec. 5.1). Then, this result is specialized to the sub-class of centrally-symmetric inclusions (Sec. 5.2), which includes the important special case of circular inclusions which is amenable to further analytical treatment (Sec. 5.3).

5.1 Small inclusion of arbitrary shape

Proposition 1. *For a penetrable inclusion represented by (26), i.e. of shape $\mathscr{B}$ and characteristic size ε, embedded in the reference medium Ω at a chosen location $\boldsymbol{a}$ in such a way that that (28) holds, the $O(\varepsilon^4)$ expansion of any objective function $J(\varepsilon)$ of format (9) with densities $\varphi_N(w,\boldsymbol{\xi})$ and $\varphi_D(w,\boldsymbol{\xi})$ twice differentiable w.r.t. their first argument is*

$$J(\varepsilon;\boldsymbol{a}) = J_4(\varepsilon;\boldsymbol{a}) + o(\varepsilon^4) \tag{54}$$

in terms of the fourth-order polynomial approximation

$$J_4(\varepsilon;\boldsymbol{a}) = J(0) + \mathcal{T}_2(\boldsymbol{a})\varepsilon^2 + \mathcal{T}_3(\boldsymbol{a})\varepsilon^3 + \mathcal{T}_4(\boldsymbol{a})\varepsilon^4, \tag{55}$$

with the coefficients $\mathcal{T}_2(\boldsymbol{a})$, $\mathcal{T}_3(\boldsymbol{a})$ and $\mathcal{T}_4(\boldsymbol{a})$ given by

$$\mathcal{T}_2(\boldsymbol{a}) = \boldsymbol{\nabla} u(\boldsymbol{a})\cdot\boldsymbol{\mathcal{A}}_{11}\cdot\boldsymbol{\nabla}\hat{u}(\boldsymbol{a}), \tag{56a}$$

$$\mathcal{T}_3(\boldsymbol{a}) = \boldsymbol{\nabla} u(\boldsymbol{a})\cdot\boldsymbol{\mathcal{A}}_{12}:\boldsymbol{\nabla}^2\hat{u}(\boldsymbol{a}) + \boldsymbol{\nabla}\hat{u}(\boldsymbol{a})\cdot\boldsymbol{\mathcal{A}}_{12}:\boldsymbol{\nabla}^2 u(\boldsymbol{a}), \tag{56b}$$

$$\begin{aligned}\mathcal{T}_4(\boldsymbol{a}) = {}& \frac{1}{2}(1-\beta)\boldsymbol{\mathcal{I}}_2:\boldsymbol{\nabla}^2[\boldsymbol{\nabla} u\cdot\boldsymbol{\nabla}\hat{u}](\boldsymbol{a}) + \frac{1}{2}\boldsymbol{\nabla} u(\boldsymbol{a})\boldsymbol{\mathcal{A}}_{13}\vdots\boldsymbol{\nabla}^3\hat{u}(\boldsymbol{a}) + \frac{1}{2}\boldsymbol{\nabla}\hat{u}(\boldsymbol{a})\boldsymbol{\mathcal{A}}_{13}\vdots\boldsymbol{\nabla}^3 u(\boldsymbol{a})\\ &+ \boldsymbol{\nabla} F(\boldsymbol{a})\cdot\boldsymbol{\mathcal{A}}_{11}\cdot\boldsymbol{\nabla}\hat{u}(\boldsymbol{a}) + \boldsymbol{\nabla}^2 u(\boldsymbol{a}):\boldsymbol{\mathcal{A}}_{22}:\boldsymbol{\nabla}^2\hat{u}(\boldsymbol{a})\\ &+ \frac{1}{2}\int_{S_N}\varphi_{N,uu}W^2\,d\Gamma + \frac{1}{2}\int_{S_D}\varphi_{D,pp}Q^2\,d\Gamma.\end{aligned} \tag{56c}$$

In (56a–c), the function F is defined by (50a), the function W is given by

$$W(\boldsymbol{x}) = \boldsymbol{\nabla}_\xi\mathcal{G}(\boldsymbol{x},\boldsymbol{a})\cdot\boldsymbol{\mathcal{A}}_{11}\cdot\boldsymbol{\nabla} u(\boldsymbol{a}) \tag{57}$$

and $Q=\boldsymbol{\nabla}W\cdot\boldsymbol{n}$, the tensor $\boldsymbol{\mathcal{I}}_2$ (geometrical inertia of the normalized inclusion $\mathscr{B}$) is given by

$$\boldsymbol{\mathcal{I}}_2=\int_{\mathscr{B}}(\bar{\boldsymbol{\xi}}\otimes\bar{\boldsymbol{\xi}})\;d\bar{V}_{\bar{\xi}}, \tag{58}$$

the constant tensors $\boldsymbol{\mathcal{A}}_{11},\boldsymbol{\mathcal{A}}_{12},\boldsymbol{\mathcal{A}}_{13},\boldsymbol{\mathcal{A}}_{22}$ are given by (51a,b) and

$$\boldsymbol{\mathcal{A}}_{13}=(1-\beta)k\int_{\mathscr{B}}\bar{\boldsymbol{\nabla}}\,\boldsymbol{\mathcal{U}}_1\otimes(\bar{\boldsymbol{\xi}}\otimes\bar{\boldsymbol{\xi}})\;d\bar{V}_{\bar{\xi}}, \tag{59a}$$

$$\boldsymbol{\mathcal{A}}_{22}=(1-\beta)k\int_{\mathscr{B}}\bar{\boldsymbol{\nabla}}\,\boldsymbol{\mathcal{U}}_2\otimes\bar{\boldsymbol{\xi}}\;d\bar{V}_{\bar{\xi}} \tag{59b}$$

in terms of solutions $\boldsymbol{\mathcal{U}}_1$, $\boldsymbol{\mathcal{U}}_2$ to equations (49a,b).

Proof. The proof is straightforward, and consists in deriving an explicit form for expansion (20). In particular, the expansion of the first integral of (20) exploits the results of Sec. 4.

(a) First integral of (20). Invoking expansion (43) of $\boldsymbol{\nabla}u_\varepsilon$, representation formulae (48a–c) for V_1,V_2,V_3, and

$$\boldsymbol{\nabla}\hat{u}(\boldsymbol{a}+\varepsilon\bar{\boldsymbol{\xi}})=\boldsymbol{\nabla}\hat{u}(\boldsymbol{a})+\varepsilon\boldsymbol{\nabla}^2\hat{u}(\boldsymbol{a})\cdot\bar{\boldsymbol{\xi}}+\frac{\varepsilon^2}{2}\boldsymbol{\nabla}^3\hat{u}(\boldsymbol{a}):(\bar{\boldsymbol{\xi}}\otimes\bar{\boldsymbol{\xi}})+o(\varepsilon^2)$$

for the adjoint field, one readily obtains

$$\begin{aligned}[\boldsymbol{\nabla}u_\varepsilon\cdot\boldsymbol{\nabla}\hat{u}](\boldsymbol{a}+\varepsilon\bar{\boldsymbol{\xi}})&=\boldsymbol{\nabla}u(\boldsymbol{a})\cdot\big[\boldsymbol{I}+\bar{\boldsymbol{\nabla}}\,\boldsymbol{\mathcal{U}}_1(\bar{\boldsymbol{\xi}})\big]\cdot\boldsymbol{\nabla}\hat{u}(\boldsymbol{a})\\&\quad+\varepsilon\Big\{\boldsymbol{\nabla}(\boldsymbol{\nabla}u\cdot\boldsymbol{\nabla}\hat{u})(\boldsymbol{a})\cdot\bar{\boldsymbol{\xi}}+\boldsymbol{\nabla}^2u(\boldsymbol{a}):\bar{\boldsymbol{\nabla}}\,\boldsymbol{\mathcal{U}}_2(\bar{\boldsymbol{\xi}})\cdot\boldsymbol{\nabla}\hat{u}(\boldsymbol{a})\\&\qquad+\boldsymbol{\nabla}u(\boldsymbol{a})\cdot\bar{\boldsymbol{\nabla}}\,\boldsymbol{\mathcal{U}}_1(\bar{\boldsymbol{\xi}})\cdot\boldsymbol{\nabla}^2\hat{u}(\boldsymbol{a})\cdot\bar{\boldsymbol{\xi}}\Big\}\\&\quad+\frac{\varepsilon^2}{2}\Big\{\boldsymbol{\nabla}^2[\boldsymbol{\nabla}u\cdot\boldsymbol{\nabla}\hat{u}](\boldsymbol{a}):(\bar{\boldsymbol{\xi}}\otimes\bar{\boldsymbol{\xi}})+\boldsymbol{\nabla}^3u(\boldsymbol{a})\vdots\bar{\boldsymbol{\nabla}}\,\boldsymbol{\mathcal{U}}_3(\bar{\boldsymbol{\xi}})\cdot\boldsymbol{\nabla}\hat{u}(\boldsymbol{a})\\&\qquad+2\boldsymbol{\nabla}F(\boldsymbol{a})\cdot\big[\boldsymbol{I}+\bar{\boldsymbol{\nabla}}\,\boldsymbol{\mathcal{U}}_1(\bar{\boldsymbol{\xi}})\big]\cdot\boldsymbol{\nabla}\hat{u}(\boldsymbol{a})+2\boldsymbol{\nabla}^2u(\boldsymbol{a}):\bar{\boldsymbol{\nabla}}\,\boldsymbol{\mathcal{U}}_2(\bar{\boldsymbol{\xi}})\cdot\boldsymbol{\nabla}^2\hat{u}(\boldsymbol{a})\cdot\bar{\boldsymbol{\xi}}\\&\qquad+\boldsymbol{\nabla}u(\boldsymbol{a})\cdot\bar{\boldsymbol{\nabla}}\,\boldsymbol{\mathcal{U}}_1(\bar{\boldsymbol{\xi}})\cdot\boldsymbol{\nabla}^3\hat{u}(\boldsymbol{a}):(\bar{\boldsymbol{\xi}}\otimes\bar{\boldsymbol{\xi}})\Big\}+o(\varepsilon^2)\end{aligned} \tag{60}$$

Integrating this expansion over B_ε, using scaled coordinates, exploiting integral identity (28) and recalling expressions (51a,b), (58) and (59a,b) of the various constant tensors, one obtains

$$\begin{aligned}(1-\beta)\int_{B_\varepsilon}k\boldsymbol{\nabla}u_\varepsilon\cdot\boldsymbol{\nabla}\hat{u}\;\mathrm{d}V_\xi&=\boldsymbol{\nabla}u(\boldsymbol{a})\cdot\boldsymbol{\mathcal{A}}_{11}\cdot\boldsymbol{\nabla}\hat{u}(\boldsymbol{a})\\&\quad+\varepsilon\Big\{\boldsymbol{\nabla}\hat{u}(\boldsymbol{a})\cdot\boldsymbol{\mathcal{A}}_{12}:\boldsymbol{\nabla}^2u(\boldsymbol{a})+\boldsymbol{\nabla}u(\boldsymbol{a})\cdot\boldsymbol{\mathcal{A}}_{12}:\boldsymbol{\nabla}^2\hat{u}(\boldsymbol{a})\Big\}\\&\quad+\frac{\varepsilon^2}{2}\Big\{(1-\beta)k\boldsymbol{\nabla}^2[\boldsymbol{\nabla}u\cdot\boldsymbol{\nabla}\hat{u}](\boldsymbol{a}):\boldsymbol{\mathcal{I}}_2+\boldsymbol{\nabla}\hat{u}(\boldsymbol{a})\cdot\boldsymbol{\mathcal{A}}_{13}\vdots\boldsymbol{\nabla}^3u(\boldsymbol{a})+\boldsymbol{\nabla}u(\boldsymbol{a})\cdot\boldsymbol{\mathcal{A}}_{13}\vdots\boldsymbol{\nabla}^3\hat{u}(\boldsymbol{a})\\&\qquad+2\boldsymbol{\nabla}F(\boldsymbol{a})\cdot\boldsymbol{\mathcal{A}}_{11}\cdot\boldsymbol{\nabla}\hat{u}(\boldsymbol{a})+2\boldsymbol{\nabla}^2u(\boldsymbol{a}):\boldsymbol{\mathcal{A}}_{22}:\boldsymbol{\nabla}^2\hat{u}(\boldsymbol{a})\Big\}\end{aligned} \tag{61}$$

(b) Second and third integrals of (20). The perturbed field v_ε at any point away from the inclusion is given by:

$$v_\varepsilon(\boldsymbol{x})=(1-\beta)\int_{B_\varepsilon}k\boldsymbol{\nabla}u_\varepsilon(\boldsymbol{\xi})\cdot\boldsymbol{\nabla}_\xi\mathcal{G}(\boldsymbol{x},\boldsymbol{\xi})\;\mathrm{d}V_\xi\qquad(\boldsymbol{x}\in\Omega\setminus B_\varepsilon). \tag{62}$$

As $\mathcal{G}(\boldsymbol{x},\boldsymbol{\xi})$ is a smooth function of $\boldsymbol{\xi}\in B_\varepsilon$ for any $\boldsymbol{x}\notin B_\varepsilon$, the leading contribution of $v_\varepsilon(\boldsymbol{x})$ as $\varepsilon\to 0$ results from a derivation formally identical to that of expansion (47), where (i) only the leading $O(\varepsilon^2)$ contribution is retained, (ii) the complementary Green's function $G_{\rm C}$ is replaced with the complete Green's function $\mathcal{G}$, and (iii) the constant tensor $\boldsymbol{\mathcal{A}}_{11}$ is introduced. This process leads to

$$v_\varepsilon(\boldsymbol{x}) = \varepsilon^2 W(\boldsymbol{x}) + o(\varepsilon^2), \qquad q_\varepsilon(\boldsymbol{x}) = \varepsilon^2 \boldsymbol{\nabla} Q(\boldsymbol{x}) + o(\varepsilon^2) \qquad (\boldsymbol{x}\in S)$$

i.e. (24), with the function W given by (57) and $Q=\boldsymbol{\nabla}W\cdot\boldsymbol{n}$. □

Remark 1. *The coefficient $\mathcal{T}_2(\boldsymbol{a})$ associated with the leading $O(\varepsilon^2)$ contribution to $J(\varepsilon)$ corresponds, as expected, to the previously known topological derivative of J, i.e. (22).*

Remark 2. *Expression (59a) of $\boldsymbol{\mathcal{A}}_{13}$ exploits identity (52b). Actual computation of $\boldsymbol{\mathcal{U}}_3$, defined by (49c) is thus not necessary, all the constant tensors featured in (56a-c) being expressed in terms of $\boldsymbol{\mathcal{U}}_1, \boldsymbol{\mathcal{U}}_2$ only.*

5.2 Centrally-symmetric inclusion

When $\mathscr{B}$ has central symmetry (i.e. is such that $\bar{\boldsymbol{\xi}}\in\mathscr{B} \Leftrightarrow -\bar{\boldsymbol{\xi}}\in\mathscr{B}$), as many simple inclusion shapes (e.g. disk, ellipse, rectangle) do, the constant tensor $\boldsymbol{\mathcal{A}}_{12}$ defined by (51b) vanishes, as shown in Appendix C. Consequently:

Proposition 2. *When the penetrable inclusion of Proposition 1 has central symmetry, expansion (54) holds with coefficients $\mathcal{T}_2, \mathcal{T}_4$ still given by (56a,c) and*

$$\mathcal{T}_3(\boldsymbol{a}) = 0, \tag{63}$$

5.3 Circular inclusion

The special case of a *circular* inclusion B_ε (where $\mathscr{B}$ is the unit disk and $|\mathscr{B}|=\pi$) is now considered. Of course, as the disk has central symmetry, simplification (63) holds, but this special case permits further analytical treatment. The constant tensor $\boldsymbol{\mathcal{I}}_2$ defined by (58) is easily found to be given by

$$\boldsymbol{\mathcal{I}}_2 = \frac{\pi}{4}\boldsymbol{I} \tag{64}$$

Moreover, integral equations (49a,b) are solvable in closed form (see Appendix B), to obtain

$$\boldsymbol{\mathcal{U}}_1 = \frac{1-\beta}{1+\beta}\,\bar{\boldsymbol{\xi}}, \qquad \boldsymbol{\mathcal{U}}_2 = \frac{1-\beta}{2(1+\beta)}\,\bar{\boldsymbol{\xi}}\otimes\bar{\boldsymbol{\xi}} + \frac{1-\beta}{4\beta}\Big(\frac{1}{1+\beta}\|\bar{\boldsymbol{\xi}}\|^2 - 1\Big)\boldsymbol{I} \qquad (\bar{\boldsymbol{\xi}}\in\mathscr{B}). \tag{65}$$

Explicit formulae for the constant tensors $\boldsymbol{\mathcal{A}}_{11}, \boldsymbol{\mathcal{A}}_{22}, \boldsymbol{\mathcal{A}}_{31}$ featured in (56a,c) then readily follow:

Lemma 6. *When the penetrable inclusion of Proposition 1 is circular, with $\mathscr{B}$ being the unit disk, the constant tensors $\boldsymbol{\mathcal{A}}_{11}, \boldsymbol{\mathcal{A}}_{22}, \boldsymbol{\mathcal{A}}_{31}$ are given by*

$$\boldsymbol{\mathcal{A}}_{11} = 2k\pi\frac{1-\beta}{1+\beta}\boldsymbol{I}\,, \quad \boldsymbol{\mathcal{A}}_{22} = \frac{k\pi}{4}\frac{(1-\beta)^2}{1+\beta}\Big(\boldsymbol{\mathcal{I}}_4 + \frac{1}{2\beta}\boldsymbol{I}\otimes\boldsymbol{I}\Big)\,, \quad \boldsymbol{\mathcal{A}}_{13} = \frac{k\pi}{4}\frac{(1-\beta)^2}{1+\beta}\boldsymbol{I}\otimes\boldsymbol{I}, \tag{66}$$

where $\boldsymbol{\mathcal{I}}_4$ is the symmetric fourth-order identity tensor, i.e. $\mathcal{I}_{ijk\ell} = (\delta_{ik}\delta_{j\ell} + \delta_{i\ell}\delta_{jk})/2$.

5.3.1 Expansion of potential inside a circular inclusion. Additionally, $\boldsymbol{\mathcal{U}}_3(\bar{\boldsymbol{\xi}})$ (which is featured in expansion (29) of the potential, but is not needed for setting up cost function expansions) is also solvable in closed form (see Appendix B), to obtain

$$\boldsymbol{\mathcal{U}}_3(\bar{\boldsymbol{\xi}}) = \frac{1-\beta}{3(1+\beta)}\Big[\,\bar{\boldsymbol{\xi}}\otimes\bar{\boldsymbol{\xi}}\otimes\bar{\boldsymbol{\xi}} + \frac{1}{4\beta}(\|\bar{\boldsymbol{\xi}}\|^2-1)\boldsymbol{\mathcal{K}}(\bar{\boldsymbol{\xi}})\,\Big] \qquad (\bar{\boldsymbol{\xi}}\in\mathscr{B}), \tag{67}$$

where $\mathcal{K}_{ijk}(\bar{\boldsymbol{\xi}}) = \delta_{jk}\bar{\xi}_i + \delta_{ki}\bar{\xi}_j + \delta_{ij}\bar{\xi}_k$.

The expansion (29), (48a–c) of the potential inside a circular inclusion takes, by virtue of (65), (66) and (67), the following more explicit form:

$$\begin{aligned} u_\varepsilon(\boldsymbol{\xi}) = u(\boldsymbol{\xi}) + \frac{1-\beta}{1+\beta}\Big\{ &\varepsilon\bar{\boldsymbol{\xi}}\cdot\boldsymbol{\nabla}u(\boldsymbol{a}) + \frac{\varepsilon^2}{2}\Big[\bar{\boldsymbol{\xi}}\cdot\boldsymbol{\nabla}^2u(\boldsymbol{a})\cdot\bar{\boldsymbol{\xi}} + 4k\pi\boldsymbol{\nabla}u(\boldsymbol{a})\cdot\boldsymbol{\nabla}G_{\mathrm{C}}(\boldsymbol{a},\boldsymbol{a})\Big] \\ &+ \frac{\varepsilon^3}{6}\Big[(\bar{\boldsymbol{\xi}}\otimes\bar{\boldsymbol{\xi}}\otimes\bar{\boldsymbol{\xi}}) \vdots \boldsymbol{\nabla}^3u(\boldsymbol{a}) + \frac{24k\pi}{1+\beta}\,\bar{\boldsymbol{\xi}}\cdot\boldsymbol{\nabla}_x\boldsymbol{\nabla}_\xi G_{\mathrm{C}}(\boldsymbol{a},\boldsymbol{a})\cdot\boldsymbol{\nabla}u(\boldsymbol{a})\Big]\Big\} + o(\varepsilon^4) \end{aligned} \tag{68}$$

5.3.2 Topological expansion of cost function. On substituting these values into (56a,c) and recalling result (63), the $O(\varepsilon^4)$ expansion of $J(\varepsilon)$ is hence given a more explicit form:

Proposition 3. *When the penetrable inclusion of Proposition 1 is circular, with $\mathscr{B}$ being the unit disk, coefficients $\mathcal{T}_2, \mathcal{T}_3, \mathcal{T}_4$ of expansion (54) are given by*

$$\mathcal{T}_2(\boldsymbol{a}) = 2k\pi\frac{1-\beta}{1+\beta}\boldsymbol{\nabla}u(\boldsymbol{a})\cdot\boldsymbol{\nabla}\hat{u}(\boldsymbol{a}) \tag{69a}$$

$$\mathcal{T}_3(\boldsymbol{a}) = 0 \tag{69b}$$

$$\begin{aligned} \mathcal{T}_4(\boldsymbol{a}) = (2\pi)^2k\Big(\frac{1-\beta}{1+\beta}\Big)^2\boldsymbol{\nabla}u(\boldsymbol{a})\cdot\boldsymbol{\nabla}_x\boldsymbol{\nabla}_\xi G_C(\boldsymbol{a},\boldsymbol{a})\cdot\boldsymbol{\nabla}\hat{u}(\boldsymbol{a}) + \frac{k\pi}{2}\frac{1-\beta}{1+\beta}\boldsymbol{\nabla}^2u(\boldsymbol{a}) \vdots \boldsymbol{\nabla}^2\hat{u}(\boldsymbol{a}) \\ + \frac{1}{2}\int_{S_N}\varphi_{N,uu}W^2\,d\Gamma + \frac{1}{2}\int_{S_D}\varphi_{D,pp}Q^2\,d\Gamma \end{aligned} \tag{69c}$$

Remark 3. *For the case of potential energy (10), the adjoint solution is simply $\hat{u} = -u/2$ by virtue of (10) and (19), and further simplification arise by virtue of (17). As a result, the $O(\varepsilon^4)$ expansion of potential energy (for a circular small inclusion) is given through*

$$\mathcal{T}_2(\boldsymbol{a}) = -k\pi\frac{1-\beta}{1+\beta}\|\boldsymbol{\nabla}u(\boldsymbol{a})\|^2, \tag{70a}$$

$$\mathcal{T}_4(\boldsymbol{a}) = -\frac{k\pi}{4}\frac{1-\beta}{1+\beta}\Big(\|\boldsymbol{\nabla}^2u(\boldsymbol{a})\|^2 + 8\pi\frac{1-\beta}{1+\beta}\boldsymbol{\nabla}u(\boldsymbol{a})\cdot\boldsymbol{\nabla}_x\boldsymbol{\nabla}_\xi G_C(\boldsymbol{a},\boldsymbol{a})\cdot\boldsymbol{\nabla}u(\boldsymbol{a})\Big) \tag{70b}$$

Remark 4. *The $O(\varepsilon^4)$ expansion of potential energy $\mathcal{E}(B_\varepsilon)$ for the case of an impenetrable inclusion (i.e. $\beta = 0$) is also considered in [15], where the proposed value for $\mathcal{T}_4$ is*

$$\mathcal{T}_4(\boldsymbol{a}) = -\frac{k\pi}{4}\big\|\boldsymbol{\nabla}^2u(\boldsymbol{a})\big\|^2 \tag{71}$$

and clearly differs from (70b) with $\beta = 0$. That (71) does not yield the correct $O(\varepsilon^4)$ contribution to the potential energy can in particular be checked on simple exact solutions for $\mathcal{E}(B_\varepsilon)$ [16] such as those given in Appendix A. Moreover, the expansion of u_ε proposed in [15] reads

$$u_\varepsilon(\boldsymbol{\xi}) = u(\boldsymbol{\xi}) + \varepsilon\bar{\boldsymbol{\xi}}\cdot\boldsymbol{\nabla}u(\boldsymbol{a}) + \frac{\varepsilon^2}{2}(\bar{\boldsymbol{\xi}}\otimes\bar{\boldsymbol{\xi}}) \vdots \boldsymbol{\nabla}^2u(\boldsymbol{a}) + o(\varepsilon^2) \tag{72}$$

(using the present notations), wherein (i) the $O(\varepsilon^2)$ contribution differs from that of (68) with $\beta=0$ and (ii) the $O(\varepsilon^3)$ contribution is lacking. Both (i) and (ii) then contribute to (71) being inexact.

6 EXTENSION TO SEVERAL SMALL INCLUSIONS

Expressions (56a–c) of $\mathcal{T}_2(\boldsymbol{a}),\mathcal{T}_3(\boldsymbol{a}),\mathcal{T}_4(\boldsymbol{a})$ are predicated on the assumption of a single inclusion characterized by its shape $\mathscr{B}$, size ε, location $\boldsymbol{a}$, and conductivity contrast β. However, this result can be extended to the case of $K>1$ inclusions $B_\varepsilon^{(m)}$ defined according to

$$B_\varepsilon^{(m)}(\boldsymbol{a}^{(m)}) = \boldsymbol{a}^{(m)} + \varepsilon\mathscr{B}^{(m)}, \quad \beta^{(m)} = k^{\star(m)}/k \qquad (1\le m\le K) \tag{73}$$

where $\boldsymbol{a}^{(m)}$ and $\mathscr{B}^{(m)}$ are the centre and (normalized) shape of the m-th inclusion, and the size parameter ε is the same for all K inclusions. To help present this generalization in a compact way, the following notational convention will be used: a superscript '(m)' attached to any previously defined symbol (e.g. $\boldsymbol{\mathcal{U}}_1^{(m)}$, $\boldsymbol{\mathcal{A}}_{11}^{(m)}$) will refer to quantities associated with the single-inclusion analysis of Secs. 4 and 5, with B_ε replaced by $B_\varepsilon^{(m)}$.

Proposition 4. *For a set of K penetrable inclusions of form (73) embedded in the reference medium Ω at prescribed locations $\boldsymbol{a}^{(1)},\dots,\boldsymbol{a}^{(K)}$, let $J(\varepsilon;\boldsymbol{a}^{(1)},\dots,\boldsymbol{a}^{(K)})$ be defined by (12), with $\Omega_\varepsilon\equiv\Omega\backslash\big(\bar B_\varepsilon^{(1)}\cup\dots\cup\bar B_\varepsilon^{(K)}\big)$ and $v_\varepsilon\equiv v_\varepsilon(\boldsymbol{\xi};\boldsymbol{a}^{(1)},\dots,\boldsymbol{a}^{(K)})$ denote the field perturbation induced by the K objects. Densities $\varphi_N(u,\boldsymbol{\xi})$, $\varphi_D(p,\boldsymbol{\xi})$ are assumed to be twice differentiable w.r.t. their first argument. The $O(\varepsilon^4)$ expansion of $J(\varepsilon)$ is*

$$J(\varepsilon;\boldsymbol{a}^{(1)},\dots,\boldsymbol{a}^{(K)}) = J(0) + \sum_{m=1}^{K} \mathcal{T}_2^{(m)}(\boldsymbol{a}^{(m)})\varepsilon^2 + \mathcal{T}_3^{(m)}(\boldsymbol{a}^{(m)})\varepsilon^3 + \hat{\mathcal{T}}_4^{(m)}(\boldsymbol{a}^{(1)},\dots,\boldsymbol{a}^{(K)})\varepsilon^4 + o(\varepsilon^4) \tag{74}$$

with $\mathcal{T}_2^{(m)}$, $\mathcal{T}_3^{(m)}$ given by (56a,b) with shape $\mathscr{B}=\mathscr{B}^{(m)}$ and contrast $\beta=\beta^{(m)}$, and $\hat{\mathcal{T}}_4^{(m)}$ given by

$$\hat{\mathcal{T}}_4^{(m)}(\boldsymbol{a}^{(1)},\dots,\boldsymbol{a}^{(K)}) = \mathcal{T}_4^{(m)}(\boldsymbol{a}^{(m)}) + \sum_{n\neq m}\boldsymbol{\nabla}F^{(n)}(\boldsymbol{a}^{(m)})\cdot\boldsymbol{\mathcal{A}}_{11}^{m}\cdot\boldsymbol{\nabla}\hat u(\boldsymbol{a}^{(m)}) + \sum_{n\neq m}\Big\{\frac{1}{2}\int_{S_N}\varphi_{N,uu}\,W^{(n)}W^{(m)}\,d\Gamma + \frac{1}{2}\int_{S_D}\varphi_{D,pp}\,Q^{(n)}Q^{(m)}\,d\Gamma\Big\} \tag{75}$$

where $F^{(n)}$ and $W^{(n)}$ are defined by (50a) and (57) with $\boldsymbol{a}=\boldsymbol{a}^{(n)}$, $\mathscr{B}=\mathscr{B}^{(n)}$ and $\beta=\beta^{(n)}$.

Proof. The $O(\varepsilon^4)$ expansion of $J(\varepsilon)$ is sought on the basis of

$$J(\varepsilon) = J(0) + \sum_{m=1}^{K}(1-\beta^{(m)})\int_{B_\varepsilon^{(m)}} m\boldsymbol{\nabla}u_\varepsilon\cdot\boldsymbol{\nabla}\hat u\,\mathrm{d}V + \frac{1}{2}\int_{S_\mathrm{D}}\varphi_{\mathrm{D},pp}\,(q_\varepsilon)^2\,\mathrm{d}\Gamma + \frac{1}{2}\int_{S_\mathrm{N}}\varphi_{\mathrm{N},uu}\,(v_\varepsilon)^2\,\mathrm{d}\Gamma + o(|v_\varepsilon|^2_{L^2(S_\mathrm{N})}\,,\,|q_\varepsilon|^2_{L^2(S_\mathrm{D})}). \tag{76}$$

(a) First integral of (76). To evaluate the first integral of (76), an expansion of u_ε in each inclusion, of the form

$$u_\varepsilon(\boldsymbol{\xi}) = u(\boldsymbol{\xi}) + \varepsilon\hat V_1^{(m)}(\bar{\boldsymbol{\xi}}) + \varepsilon^2\hat V_2^{(m)}(\bar{\boldsymbol{\xi}}) + \varepsilon^3\hat V_3^{(m)}(\bar{\boldsymbol{\xi}}) + o(\varepsilon^3) \qquad (\boldsymbol{\xi}\in B_\varepsilon^{(m)},\bar{\boldsymbol{\xi}}\in\mathscr{B}^{(m)}) \tag{77}$$

is again postulated. It is expected that $(\hat{V}_1^{(m)}, \hat{V}_2^{(m)}, \hat{V}_3^{(m)}) \neq (V_1^{(m)}, V_2^{(m)}, V_3^{(m)})$ because of coupling effects between inclusions. The governing integral equation for v_ε is (31) with all integrals over Γ_ε changed to sums of integrals over the $\Gamma_\varepsilon^{(m)}$, i.e.

$$\begin{aligned} u_\varepsilon(\boldsymbol{x}) - (1-\beta^{(m)})k \int_{B_\varepsilon^{(m)}} \boldsymbol{\nabla} u_\varepsilon(\boldsymbol{\xi}) \cdot \boldsymbol{\nabla}_\xi \mathcal{G}(\boldsymbol{x}, \boldsymbol{\xi}) \, \mathrm{d}V_\xi \\ - \sum_{n \neq m} (1-\beta^{(n)})k \int_{B_\varepsilon^{(n)}} \boldsymbol{\nabla} u_\varepsilon(\boldsymbol{\xi}) \cdot \boldsymbol{\nabla}_\xi \mathcal{G}(\boldsymbol{x}, \boldsymbol{\xi}) \, \mathrm{d}V_\xi = u(\boldsymbol{x}) \qquad (\boldsymbol{x} \in B_\varepsilon^{(m)}, 1 \leq m \leq K). \end{aligned} \tag{78}$$

The $(\hat{V}_1^{(m)}, \hat{V}_2^{(m)}, \hat{V}_3^{(m)})$ are to be found by inserting (77) into the first integral of (78) and expanding the resulting equations in powers of ε. A comparison with (31) indicates that the first line in (78) constitutes the contribution to the governing linear operator arising due to inclusion $B_\varepsilon^{(m)}$ in isolation. The expansion in ε of that contribution therefore coincides with that established in section 4 for the single-inclusion case. Besides, the sum of integrals in the second line of (78), which synthesizes the influence of scatterers $B_\varepsilon^{(n)}$ $(n \neq m)$ to v_ε on $B_\varepsilon^{(m)}$, can readily be shown by means of a calculation similar to that leading to (47) to have the expansion

$$\begin{aligned} \sum_{n \neq m} (1-\beta^{(n)})k \int_{B_\varepsilon^{(n)}} \boldsymbol{\nabla} u_\varepsilon(\boldsymbol{\xi}) \cdot \boldsymbol{\nabla}_\xi \mathcal{G}(\boldsymbol{x}, \boldsymbol{\xi}) \, \mathrm{d}V_\xi \\ = \sum_{n \neq m} \Big\{ \varepsilon^2 F^{(n)}(\boldsymbol{a}^{(m)}) + \varepsilon^3 \big(\boldsymbol{\nabla} F^{(n)}(\boldsymbol{a}^{(m)}) + G^{(n)}(\boldsymbol{a}^{(m)}) \big) \Big\} + o(\varepsilon^3) \qquad (\boldsymbol{x} \in B_\varepsilon^{(m)}) \end{aligned} \tag{79}$$

where the scalar functions $F^{(n)}(\boldsymbol{x})$, $G^{(n)}(\boldsymbol{x})$ are defined for any $\boldsymbol{x} \neq \boldsymbol{a}^{(n)}$ by

$$F^{(n)}(\boldsymbol{x}) = \boldsymbol{\nabla} u(\boldsymbol{a}^{(n)}) \cdot \boldsymbol{\mathcal{A}}_{11}^{(n)} \cdot \boldsymbol{\nabla} G_{\mathrm{C}}(\boldsymbol{x}, \boldsymbol{a}^{(n)}) \tag{80a}$$

$$G^{(n)}(\boldsymbol{x}) = \boldsymbol{\nabla} u(\boldsymbol{a}^{(n)}) \cdot \boldsymbol{\mathcal{A}}_{12}^{(n)} : \boldsymbol{\nabla}^2 G_{\mathrm{C}}(\boldsymbol{x}, \boldsymbol{a}^{(n)}) + \boldsymbol{\nabla} G_{\mathrm{C}}(\boldsymbol{x}, \boldsymbol{a}^{(n)}) \cdot \boldsymbol{\mathcal{A}}_{12}^{(n)} : \boldsymbol{\nabla}^2 u(\boldsymbol{a}^{(n)}), \tag{80b}$$

Since contributions (79) are of order $O(\varepsilon^2)$, the $O(\varepsilon)$ contributions to equation (78) are not affected by the scatterers $B_\varepsilon^{(n)}$ $(n \neq m)$, and one therefore has

$$\hat{V}_1^{(n)}(\bar{\boldsymbol{\xi}}) = V_1^{(n)}(\bar{\boldsymbol{\xi}}) \qquad (\bar{\boldsymbol{\xi}} \in \mathscr{B}^{(n)}) \tag{81}$$

Moreover, the form assumed by the supplementary contributions (79) is such that results of section 3.3 still apply provided every occurrence of $F(\boldsymbol{a})$ and $G(\boldsymbol{a})$ is replaced by $\hat{F}^{(m)}(\boldsymbol{a}^{(m)})$ and $\hat{G}^{(m)}(\boldsymbol{a}^{(m)})$, respectively, where

$$\begin{aligned} \hat{F}^{(m)}(\boldsymbol{a}^{(m)}) &= F^{(m)}(\boldsymbol{a}^{(m)}) + \sum_{n \neq m} F^{(n)}(\boldsymbol{a}^{(m)}), \\ \hat{G}^{(m)}(\boldsymbol{a}^{(m)}) &= G^{(m)}(\boldsymbol{a}^{(m)}) + \sum_{n \neq m} G^{(n)}(\boldsymbol{a}^{(m)}). \end{aligned} \tag{82}$$

The supplementary terms (contributions of $B_\varepsilon^{(n)}$, $n \neq m$) are the only manifestations of interactions between inclusions arising in this analysis. The auxiliary unknowns $\hat{V}_2^{(m)}, \hat{V}_3^{(m)}$ are then given

by (48b,c) with replacements (82), i.e. by

$$\hat{V}_2^{(m)}(\bar{\boldsymbol{\xi}}) = V_2^{(m)}(\bar{\boldsymbol{\xi}}) + \sum_{n\neq m} F^{(n)}(\boldsymbol{a}^{(m)}), \tag{83a}$$

$$\hat{V}_3^{(m)}(\bar{\boldsymbol{\xi}}) = V_3^{(m)}(\bar{\boldsymbol{\xi}}) + 2\sum_{n\neq m} \big[\bar{\boldsymbol{\xi}} + \boldsymbol{\mathcal{U}}_1^{(n)}(\bar{\boldsymbol{\xi}})\big]\cdot\boldsymbol{\nabla} F^{(n)}(\boldsymbol{a}^{(m)}) + 2G^{(n)}(\boldsymbol{a}^{(m)}) \tag{83b}$$

(b) Second and third integrals of (76). On noting that the integral representation (62) is a sum of integrals over each inclusion and revisiting the analysis of section 5, the leading $O(\varepsilon^2)$ contribution to v_ε is simply the corresponding sum of contributions (24), i.e.:

$$v_\varepsilon(\boldsymbol{\xi}) = \varepsilon^2 \sum_{m=1}^{K} W^{(m)}(\boldsymbol{\xi}) + o(\varepsilon^2)\,, \qquad q_\varepsilon(\boldsymbol{\xi}) = \varepsilon^2 \sum_{m=1}^{K} Q^{(m)}(\boldsymbol{\xi}) + o(\varepsilon^2) \qquad (\boldsymbol{\xi}\in S) \tag{84}$$

where $W^{(m)}$ is defined by (57). The leading contribution of the last two integrals of (76), of order $O(\varepsilon^4)$, then stems directly from estimates (84).

(c) Proof. Proposition 4 then follows from collecting results (76), (81), (82), (83a,b) and (84) and revisiting the analysis of Secs. 4 and 5. □

7 DISCUSSION

7.1 Computational issues

The developments of sections 3 to 6 are based on the Green's function $\mathcal{G}$ defined by (30), and lead to almost explicit formulae for the $O(\varepsilon^4)$ expansion of $J(\varepsilon)$ (their only non-explicit components being the auxiliary solutions $\boldsymbol{\mathcal{U}}_1, \boldsymbol{\mathcal{U}}_2$, which must be computed numerically except for simple normalized inclusion $\mathscr{B}$ shape such as the circular shape discussed in section 5.3).

In practice, this explicit character is retained only for geometries Ω and boundary conditions settings $S_{\rm N}, S_{\rm D}$ such that the corresponding Green's function is known analytically. Such cases are limited to geometrically simple configurations. For instance, for the half-plane $\Omega = \{\boldsymbol{\xi}\,|\,\xi_2 \le 0\}$ bounded by $S = \{\boldsymbol{\xi}\,|\,\xi_2 = 0\}$, it is well-known that

$$G_{\rm C}(\boldsymbol{x},\boldsymbol{\xi}) = \mp\frac{1}{2\pi}{\rm Log}\tilde{r}, \qquad \text{with } \tilde{r} = \|\boldsymbol{\xi} - \tilde{\boldsymbol{x}}\|\,,\ \ \tilde{\boldsymbol{x}} = (x_1, -x_2) \tag{85}$$

where the '-' and '+' sign correspond to the cases $S_{\rm N} = S$, $S_{\rm D} = \emptyset$ (Neumann) and $S_{\rm D} = S$, $S_{\rm N} = \emptyset$ (Dirichlet). Another configuration with a known (and relatively simple) Green's function is the circular disk, see Eq. (A.1).

For configurations where the Green's function is not available, the free and adjoint fields, defined

by (6) and (19), may be computed by solving the boundary integral equations [21, 22]

$$\big[\mathcal{L}(u,p)\big](\boldsymbol{x}) = \big[\mathcal{F}(u^{\mathrm{D}},p^{\mathrm{D}})\big](\boldsymbol{x}) \qquad (\boldsymbol{x}\in S) \tag{86}$$

$$\big[\mathcal{L}(\hat{u},\hat{p})\big](\boldsymbol{x}) = \big[\mathcal{F}(-\varphi_{\mathrm{D},p},\varphi_{\mathrm{N},u})\big](\boldsymbol{x}) \qquad (\boldsymbol{x}\in S) \tag{87}$$

with the integral operator $\mathcal{L}(f,g)$ and right-hand side functional $\mathcal{F}(f^{\mathrm{D}},g^{\mathrm{D}})$ defined by

$$\big[\mathcal{K}(f,g)\big](\boldsymbol{x}) = \frac{1}{2}f(\boldsymbol{x}) + \int_{S_{\mathrm{N}}} H(\boldsymbol{x},\boldsymbol{\xi})f(\boldsymbol{\xi})\,\mathrm{d}\Gamma_\xi - \int_{S_{\mathrm{D}}} G(\boldsymbol{x},\boldsymbol{\xi})g(\boldsymbol{\xi})\,\mathrm{d}\Gamma_\xi \qquad (\boldsymbol{x}\in S), \tag{88a}$$

$$\big[\mathcal{F}(f^{\mathrm{D}},g^{\mathrm{D}})\big](\boldsymbol{x}) = -\int_{S_{\mathrm{D}}} H(\boldsymbol{x},\boldsymbol{\xi})f^{\mathrm{D}}(\boldsymbol{\xi})\,\mathrm{d}\Gamma_\xi + \int_{S_{\mathrm{N}}} G(\boldsymbol{x},\boldsymbol{\xi})g^{\mathrm{D}}(\boldsymbol{\xi})\,\mathrm{d}\Gamma_\xi \qquad (\boldsymbol{x}\in S), \tag{88b}$$

and subsequently invoking integral representation formulae. Moreover, the pair (W,Q) associated with the leading $O(\varepsilon^2)$ contribution of $(v_\varepsilon,q_\varepsilon)$ on S, defined by (57), and the complementary kernel pair $G_{\mathrm{C}}(\boldsymbol{z},\boldsymbol{\xi})$, defined by (37) and featured in $\mathcal{T}_4$, are respectively governed by integral equations

$$\big[\mathcal{L}(W,Q)\big](\boldsymbol{x}) = -\boldsymbol{\nabla}u(\boldsymbol{a})\cdot\boldsymbol{\mathcal{A}}_{11}\cdot\boldsymbol{\nabla}G(\boldsymbol{x},\boldsymbol{a}) \qquad (\boldsymbol{x}\in S) \tag{89}$$

$$\big[\,\mathcal{L}\big(G_{\mathrm{C}}(\boldsymbol{z},\cdot),\,H_{\mathrm{C}}(\boldsymbol{z},\cdot)\big)\,\big](\boldsymbol{x}) = -\big[\,\mathcal{F}\big(G(\boldsymbol{z},\cdot),\,H(\boldsymbol{z},\cdot)\big)\,\big](\boldsymbol{x}) \qquad (\boldsymbol{x}\in S,\boldsymbol{z}\in\Omega) \tag{90}$$

where $H_{\mathrm{C}}(\boldsymbol{z},\boldsymbol{\xi}) = k\boldsymbol{\nabla}_\xi G_{\mathrm{C}}(\boldsymbol{z},\boldsymbol{\xi})\cdot\boldsymbol{n}(\boldsymbol{\xi})$.

Alternatively, finite element methods (FEMs) may also be used for setting up expansions of the form (54). Coefficient $\mathcal{T}_2$ is similar to an energy density, and as such may be computed using the FEM in its standard form. On the other hand, coefficient $\mathcal{T}_4$ entails computing second-order gradients of the free and adjoint fields, which normally requires specially-designed procedures and raises accuracy issues (while integral representations of second-order gradients do not).

7.2 Direct vs. adjoint approaches for topological sensitivity

Topological sensitivity has formal similarities with the more traditional areas of parameter sensitivity [1] or shape sensitivity [2]. Like first-order parameter or shape sensitivity formulae, the topological derivative $\mathcal{T}_2$ associated with the leading $O(\varepsilon^2)$ contribution to $J(\varepsilon)$ is expressed as a bilinear combination of the free and adjoint fields. Moreover, setting up the $O(\varepsilon^4)$ expansion of $J(\varepsilon)$, and particularly the highest-order coefficient $\mathcal{T}_4$, requires the 'direct topological field sensitivities' W,Q, in addition to the free and adjoint fields. This is reminiscent of the fact that second-order parameter or shape sensitivity fomulae can be cast as bilinear combinations of the free and adjoint fields and their first-order sensitivities. One nevertheless has to keep in mind that topological and shape sensitivities are related but distinct concepts, as emphasized in [23].

Here, it would have been possible to establish the $O(\varepsilon^4)$ expansion of $J(\varepsilon)$ on the basis of (15) rather than (20), without recourse to the adjoint solution (19). This alternative 'direct' approach requires $O(\varepsilon^4)$ expansions of v_ε on S_{N} and q_ε on S_{D}, i.e. the actual computation of higher-order direct topological field sensitivities W_2,W_3 in addition to $W=W_1$ defined in (24). The latter can

be obtained by expanding integral representation (34) to order $O(\varepsilon^4)$. General explicit formulae for such high-order expansions of the field quantities are given, to arbitrary order and for various physical contexts, by Ammari and Kang [13] in terms of the Green's function (30) and its derivatives.

8 NUMERICAL EXAMPLES

Numerical experiments on higher-order topological sensitivity have been performed on the following configuration (Fig. 1), previously used in [15]. The reference domain Ω is defined by $\Omega =]0,1[\times]0,1[$. The boundary conditions are as follows: a potential $u^{\mathrm{D}} = 0$ is applied on $S_{\mathrm{D}}^{(1)}$ and $S_{\mathrm{D}}^{(2)}$, and a flux $p_1^{\mathrm{D}} = 1$ on $S_{\mathrm{N}}^{(1)}$ and $p_2^{\mathrm{D}} = 2$ on $S_{\mathrm{N}}^{(2)}$. The remaining part $S \setminus (S_{\mathrm{D}}^{(1)} \cup S_{\mathrm{D}}^{(2)} \cup S_{\mathrm{N}}^{(1)} \cup S_{\mathrm{N}}^{(2)})$ of the boundary is insulated ($p^{\mathrm{D}} = 0$). Numerical experiments on the $O(\varepsilon^4)$ expansion of potential energy (9), (10), including comparisons with results using the defective $O(\varepsilon^4)$ term of [15], are first reported in Sec. 8.1. Then, the usefulness of the $O(\varepsilon^4)$ expansion of least-squares output misfit function (9), (11) for computationally-fast identification of buried inclusions is demonstrated in Sec. 8.2

Solutions u and $(u^\star, u^\star)$, corresponding to reference domain and perturbed configurations with one penetrable inclusion of finite size, are computed using a standard boundary element method (BEM), with piecewise-linear and piecewise-constant interpolations, respectively, for potentials and fluxes on boundaries and interfaces. As the Green's function for the domain is not known in closed form, the complementary part G_{C} of the Green's function is numerically evaluated by solving a BEM-discretized version of integral equation (90) with $\boldsymbol{z}$ taken in turn as each sampling point $\boldsymbol{a} \in \mathbf{G}$. As the integral operator $\mathcal{L}$ in (90) does not depend on $\boldsymbol{z}$, this only entails computing a right-hand side and performing a backsubstitution for each $\boldsymbol{a} \in \mathbf{G}$, and hence defines a computationally reasonable task even for a dense search grid $\mathbf{G}$.

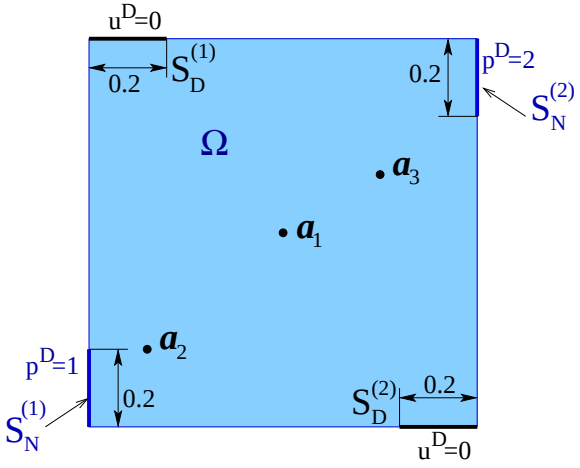

Figure 1: *Numerical examples: geometry and boundary conditions for reference configuration.*

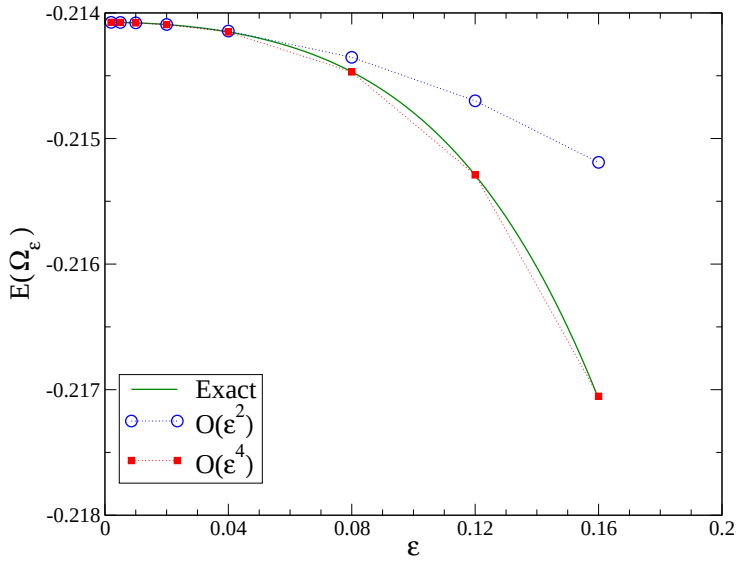

Figure 2: *Small-inclusion expansion of potential energy: circular hole ($\beta = 0$) located at* $\boldsymbol{a}_1 = (1/2,\, 1/2)$.

8.1 Small-inclusion expansion of potential energy

In this section, the cost function is the potential energy $\mathcal{E}(B^\star)$, which for this example is given by

$$\mathcal{E}(B^\star) = \frac{1}{2}\int_{S_{\mathrm{N}}^{(1)}} u^\star \,\mathrm{d}\Gamma + \int_{S_{\mathrm{N}}^{(2)}} u^\star \,\mathrm{d}\Gamma$$

First, the case of an impenetrable circular inclusion ($\beta = 0$) located at $\boldsymbol{a}_1 = (1/2,\, 1/2)$ is considered. The correct value of $\mathcal{E}(B_\varepsilon)$ for $0 < \varepsilon \leq 0.16$ is compared on Fig. 2 to the $O(\varepsilon^2)$ and $O(\varepsilon^4)$ expansions obtained using (55) and (69a–c) with $\beta = 0$. The $O(\varepsilon^4)$ expansion is seen to approximate $\mathcal{E}(B_\varepsilon)$ very

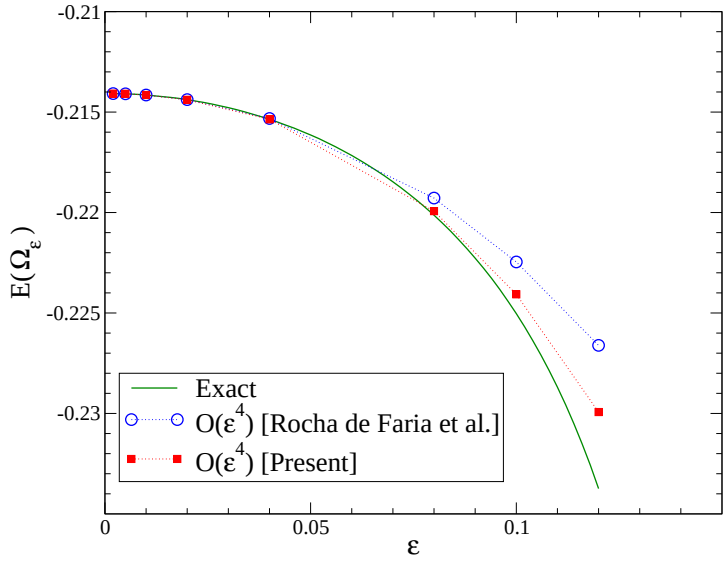

Figure 3: *Small-inclusion expansion of potential energy: circular hole ($\beta = 0$) located at* $\boldsymbol{a}_2 = (0.15,\, 0.2)$.

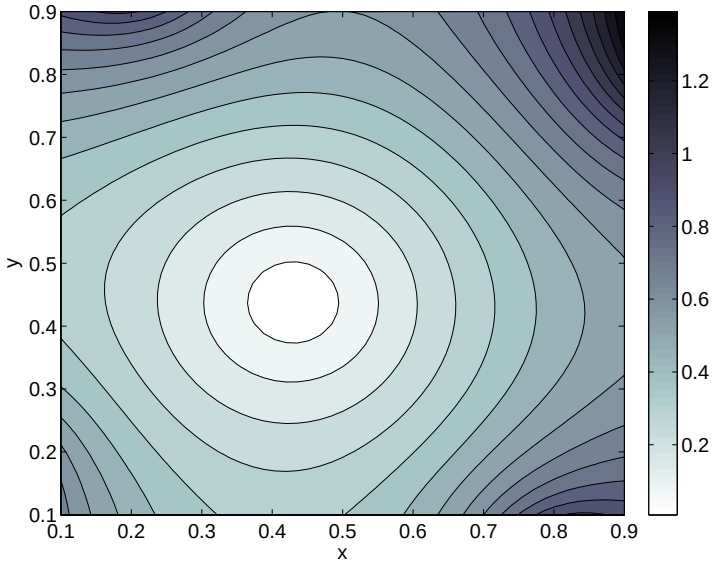

Figure 4: *Small-inclusion expansion of potential energy: distribution of* $\|\boldsymbol{\nabla} u\|^2$ *over* Ω.

well for the considered range of inclusion sizes, while as expected the $O(\varepsilon^2)$ expansion performs well over a narrower inclusion size range (note that for the largest value $\varepsilon = 0.16$ the inclusion is relatively large as its diameter is nearly one-third of the overall domain linear size). This example (with the same inclusion location) was also considered in [15], where the $O(\varepsilon^4)$ expansion computed on the basis of (71), which is missing a term proportional to $\boldsymbol{\nabla} u(\boldsymbol{a}) \cdot \boldsymbol{\nabla}_x \boldsymbol{\nabla}_\xi G_{\mathrm{C}}(\boldsymbol{a}, \boldsymbol{a}) \cdot \boldsymbol{\nabla} u(\boldsymbol{a})$, was found to perform similarly well. In contrast, a comparison of the results obtained for the inclusion location $\boldsymbol{a}_2 = (0.15,\, 0.2)$ using either the present expression (70b) of $\mathcal{T}_4$ or (71) reveals a noticeably larger error when using the latter (see Fig. 3). The higher discrepancy in the latter case

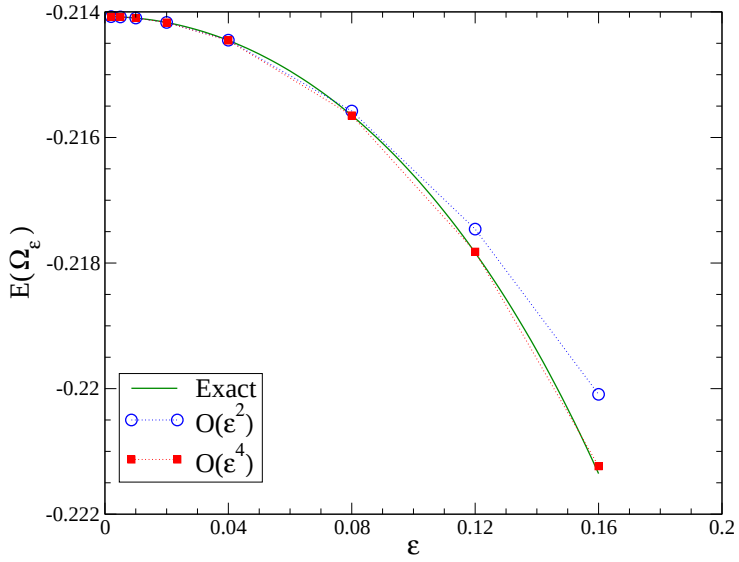

Figure 5: *Small-inclusion expansion of potential energy: circular penetrable inclusion* ($\beta = 0.6$) *located at* $\boldsymbol{a}_3 = (0.75,\, 0.65)$.

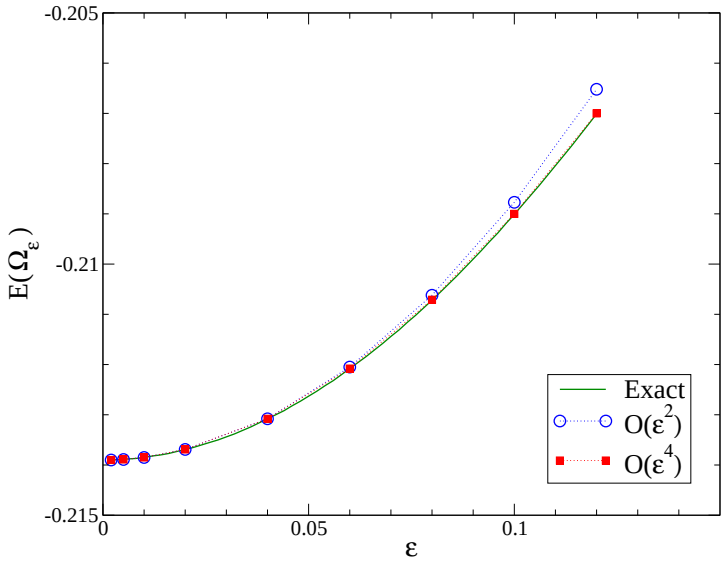

Figure 6: *Small-inclusion expansion of potential energy: circular penetrable inclusion ($\beta = 5$) located at $\boldsymbol{a}_2 = (0.15,\ 0.2)$.*

stems from the combined effect on the value taken by $\boldsymbol{\nabla} u(\boldsymbol{a}) \cdot \boldsymbol{\nabla}_x \boldsymbol{\nabla}_\xi G_{\rm C}(\boldsymbol{a}, \boldsymbol{a}) \cdot \boldsymbol{\nabla} u(\boldsymbol{a})$ of (i) the complementary Green's function and its gradients taking larger values closer to the boundary (here $\|\boldsymbol{\nabla}_x \boldsymbol{\nabla}_\xi G_{\rm C}(\boldsymbol{a}_1, \boldsymbol{a}_1)\| \approx .543$ but $\|\boldsymbol{\nabla}_x \boldsymbol{\nabla}_\xi G_{\rm C}(\boldsymbol{a}_2, \boldsymbol{a}_2)\| \approx 3.95$) and (ii) $\|\boldsymbol{\nabla} u(\boldsymbol{a}_1)\|$ happening to be significantly smaller than $\|\boldsymbol{\nabla} u(\boldsymbol{a}_2)\|$ (see Fig. 4).

Next, the case of a penetrable circular inclusion ($\beta = 0.6$) located at $\boldsymbol{a}_3 = (0.75,\ 0.65)$ is considered. The correct value of $\mathcal{E}(B_\varepsilon)$ for $0 < \varepsilon \leq 0.16$ is compared on Fig. 5 to the present $O(\varepsilon^2)$ and $O(\varepsilon^4)$ expansions based on a small circular inclusion with $\beta = 0.6$. Finally, the same comparison is performed on Fig. 6 for the case of a penetrable circular inclusion ($\beta = 5$) located at $\boldsymbol{a}_2 = (0.15,\ 0.2)$, for inclusion sizes such that $0 < \varepsilon < 0.12$. In both cases, the present $O(\varepsilon^4)$ expansion is seen to provide a very good approximation of $\mathcal{E}(B_\varepsilon)$. Note that the largest size $\varepsilon = 0.12$ considered in the latter case corresponds to a relatively large inclusion which is very close to the external boundary.

8.2 Computationally-fast identification of hidden inclusion

Now, the inverse problem consisting of identifying a buried inclusion (with geometrical support $B^{\rm true}$ and conductivity contrast $\beta^{\rm true}$) from measurements on the boundary is considered, with the same example geometry and boundary conditions as before. It is in addition assumed that the overdetermined boundary data used for inclusion identification consists of a known value $u^{\rm obs}$ of potential u over the complete Neumann surface $S_{\rm N}$. The output least-squares misfit function is thus

$$\mathcal{J}_{\rm LS}(B^\star) = \frac{1}{2} \int_{S_{\rm N}} \left| u^\star(\boldsymbol{\xi}) - u^{\rm obs}(\boldsymbol{\xi}) \right|^2 \, {\rm d}\Gamma,$$

i.e. corresponds to $\varphi_{\rm N}$ defined by (11) and $\varphi_{\rm D} = 0$. Of course, the data $u^{\rm obs}$ could be used for inclusion identification purposes in many other ways. The purpose of this example is to demonstrate the usefulness of a $O(\varepsilon^4)$ expansion of $\mathcal{J}_{\rm LS}$ for fast, non-iterative identification of a hidden inclusion.

8.2.1 Approximate global search procedure. Define a fine search grid $\mathbf{G}$, i.e. a (dense) discrete set of sampling points $\boldsymbol{a}$ spanning (part of) the interior of Ω. To minimize w.r.t. ε an expansion of the form (54) of $\mathcal{J}_{\rm LS}$ at a given sampling point is a simple and computationally very light task that can be easily performed for all $\boldsymbol{a} \in \mathbf{G}$, thereby defining an approximate global search procedure over the spatial region thus sampled. The best estimate of the unknown inclusion $B^{\rm true}$ yielded by this procedure is defined by the location $\boldsymbol{a} = \boldsymbol{x}^{\rm est}$ and size $\varepsilon = R^{\rm est}$ achieving the lowest value of $J_4(\varepsilon; \boldsymbol{a})$ over $\mathbf{G}$, i.e. given by

$$\boldsymbol{x}^{\rm est} = \arg\min_{\boldsymbol{a}\in\mathbf{G}} J^{\rm min}(\boldsymbol{a}), \qquad R^{\rm est} = R(\boldsymbol{x}^{\rm est}), \tag{91}$$

with functions $J^{\rm min}(\boldsymbol{a})$ and $R(\boldsymbol{a})$ defined through a partial minimization of $J_4(\varepsilon; \boldsymbol{a})$ w.r.t. ε, i.e.:

$$J^{\rm min}(\boldsymbol{a}) = \min_{\varepsilon} J_4(\varepsilon; \boldsymbol{a}), \qquad R(\boldsymbol{a}) = \arg\min_{\varepsilon} J_4(\varepsilon; \boldsymbol{a}). \tag{92}$$

The estimated location $\boldsymbol{x}^{\rm est}$ and size $R^{\rm est}$ can then be used as either an stand-alone estimate of the sought inclusion or as an initial guess for a subsequent refined inversion algorithm. The constitutive characteristics of the inclusion are assumed (i.e. not treated as unknowns in the search). The influence of such assumption on the accuracy of estimates $\boldsymbol{x}^{\rm est}$, $R^{\rm est}$ is examined in the last part of this section.

The definition (92) of function $J^{\rm min}(\boldsymbol{a})$ is valid only at sampling points $\boldsymbol{a}$ where $\mathcal{T}_2(\boldsymbol{a}) \leq 0$ and $\mathcal{T}_4(\boldsymbol{a}) > 0$ (assuming the trial inclusion to be centrally-symmetric), as $J_4(\varepsilon; \boldsymbol{a})$ (i) has no lower bound if $\mathcal{T}_4(\boldsymbol{a}) < 0$, or (ii) is minimum at $\varepsilon = 0$ if $\mathcal{T}_2(\boldsymbol{a}) \geq 0$ and $\mathcal{T}_4(\boldsymbol{a}) > 0$. These conditions were found to be met at all $\boldsymbol{a} \in \mathbf{G}$ for all of the following examples.

8.2.2 Numerical results for inclusion identification. The above-described approximate global search procedure is here applied to the identification, from simulated data, of an inclusion centered at $\boldsymbol{x}^{\rm true} = (0.41,\, 0.595)$. This inclusion location (remote from the boundary, and in particular from the region where fluxes are applied) was chosen so as to test the proposed approximate global search procedure on a case where the boundary data is rather insensitive to details of the inclusion shape. Three inclusion shapes are considered: a circular inclusion with radius $R^{\rm true} = 0.06$ (inclusion 1), an elliptical inclusion with semiaxes $(A^{\rm true}, B^{\rm true}) = (0.06,\, 0.015)$ and principal axes rotated by $\pi/6$ (inclusion 2) and $2\pi/3$ (inclusion 3). For each inclusion, three possibilities of conductivity contrast $\beta_a^{\rm true} = 0$, $\beta_b^{\rm true} = 0.6$, $\beta_c^{\rm true} = 3.5$ are considered, and synthetic data $u^{\rm obs}$ is computed for each case (using again a BEM model with 100 elements on S and 100 on $\Gamma^\star$). This defines overall nine configurations of unknown inclusions, labelled 1a to 3c. A search grid $\mathbf{G}$ of 51×51 regularly spaced

sampling points covering the square region $0.1 \leq x_1, x_2 \leq 0.9$ is defined (the grid spacing is hence $\Delta x_1 = \Delta x_2 = 0.016$).

Identification using noise-free synthetic data. A first set of results was obtained by assuming knowledge of the correct value β^{true} of conductivity contrast of the inclusion. Results obtained in terms of $\boldsymbol{x}^{\text{est}}$ and R^{est} for all nine configurations 1a to 3c for noise-free synthetic data are given in Table 1. For comparison purposes, the 'true' radius R^{true} is defined as the radius of the disk having the same area as B^{true}, i.e. $R^{\text{true}} = 0.06$ for inclusion 1 and $R^{\text{true}} = 0.03$ for inclusions 2,3. Additionally, the function $J^{\min}(\boldsymbol{a})$, shown together with the outline of B^{true} on Figs. 7, 8, 9, is seen in all cases to attain values close to its global minimum only in the vicinity of the actual inclusion.

Identification using noisy synthetic data. The effect of imperfect data is now tested, for inclusion 3, by defining a perturbed version u_σ^{obs} of u^{obs} according to

$$u_\sigma^{\text{obs}} = u^{\text{obs}} + \sigma\chi\|u - u^{\text{obs}}\|_{L^2(S_{\text{N}})}$$

where χ is a uniform random variable with zero mean and unit standard deviation, and σ is here set to 0.2. Results obtained in terms of $\boldsymbol{x}^{\text{est}}$ and R^{est} and of the function $J^{\min}(\boldsymbol{a})$, respectively shown in Table 2 and Fig. 10, are very similar to the corresponding ones for noise-free data. The proposed approximate global search method thus appears to be only moderately sensitive to the adverse effect of measurement noise.

Influence of the conductivity contrast. Finally, the approximate global search procedure based on $J_4(\varepsilon; \boldsymbol{a})$ has been performed on configurations 1a, 1b and 1c for values of β spanning the interval

inclusion 1	$\beta_a^{\text{true}} = 0$	$\beta_b^{\text{true}} = 0.6$	$\beta_c^{\text{true}} = 5$
$\boldsymbol{x}^{\text{est}}$	(0.404, 0.596)	(0.404, 0.596)	(0.420, 0.596)
R^{est}	6.15e-02	6.06e-02	5.89e-02
inclusion 2	$\beta_a^{\text{true}} = 0$	$\beta_b^{\text{true}} = 0.6$	$\beta_c^{\text{true}} = 5$
$\boldsymbol{x}^{\text{est}}$	(0.404, 0.580)	(0.404, 0.596)	(0.420, 0.596)
R^{est}	2.42e-02	2.82e-02	3.63e-02
inclusion 3	$\beta_a^{\text{true}} = 0$	$\beta_b^{\text{true}} = 0.6$	$\beta_c^{\text{true}} = 5$
$\boldsymbol{x}^{\text{est}}$	(0.404, 0.596)	(0.420, 0.596)	(0.404, 0.596)
R^{est}	4.80e-02	3.22e-02	2.61e-02

Table 1: *Identification of buried circular or elliptical inclusion: estimated location $\boldsymbol{x}^{est}$ and size R^{est} (noise-free synthetic data); reference values are $R^{true} = 0.06$ (inclusion 1), $R^{true} = 0.03$ (inclusions 2,3) and $\boldsymbol{x}^{true} = (0.41,\ 0.595)$.*

inclusion 3	$\beta_a^{\text{true}} = 0$	$\beta_b^{\text{true}} = 0.6$	$\beta_c^{\text{true}} = 5$
$\boldsymbol{x}^{\text{est}}$	(0.404, 0.596)	(0.404, 0.612)	(0.404, 0.596)
R^{est}	4.78e-02	3.28e-02	2.62e-02

Table 2: *Identification of inclusion 3 (elliptical): estimated location $\boldsymbol{x}^{est}$ and size R^{est}, (noisy synthetic data, with 20% noise on $u^{obs} - u$); reference values are $R^{true} = 0.03$ and $\boldsymbol{x}^{true} = (0.41,\ 0.595)$.*

$0 \le \beta \le 5$ to examine the effect of incorrect assumed values of β on the method. The estimated location $\boldsymbol{x}^{\text{est}}$ as given in Table 1 was obtained for all β in the following intervals: $0 \le \beta \le 0.5$ (inclusion 1a), $0 \le \beta \le 0.7$ (inclusion 1b) and $1.5 \le \beta \le 5$ (inclusion 1c); in addition, $\beta = 0.8,\ 0.9$ yielded $\boldsymbol{x}^{\text{est}} = (0.420, 0.596)$ for inclusion 1b. In other words, the inclusion is acceptably located for large ranges of trial values of β containing the correct value β^{true}. The estimated size R^{est} was found to depend on the assumed value of β. Indeed, expressions (56a–c) of $\mathcal{T}_2, \mathcal{T}_4$ suggest that the expansion is primarily sensitive to the value of combination $\boldsymbol{\mathcal{A}}_{11}\varepsilon^2$, where $\boldsymbol{\mathcal{A}}_{11}$ is the polarization tensor (51a); note in particular that W and Q depend linearly on $\boldsymbol{\mathcal{A}}_{11}$, see (57). For the case of a circular trial inclusion, expansion $J_4(\varepsilon; \boldsymbol{a})$ can indeed be put in the form

$$J_4(\varepsilon; \boldsymbol{a}) = aC(\varepsilon, \beta) + bC^2(\varepsilon, \beta) + cC(\varepsilon, \beta)\varepsilon^2, \qquad C(\varepsilon, \beta) = \frac{1-\beta}{1+\beta}\varepsilon^2 \tag{93}$$

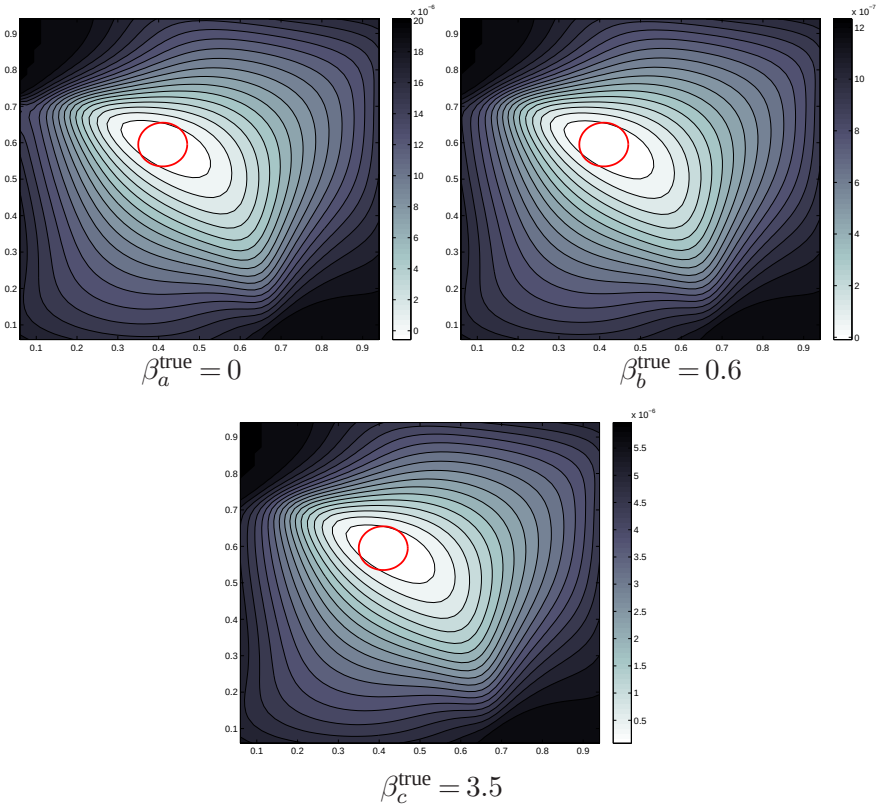

Figure 7: *Identification of inclusion 1 (circular): distribution of J^{min} over search grid* **G**, *and outline of true inclusion.*

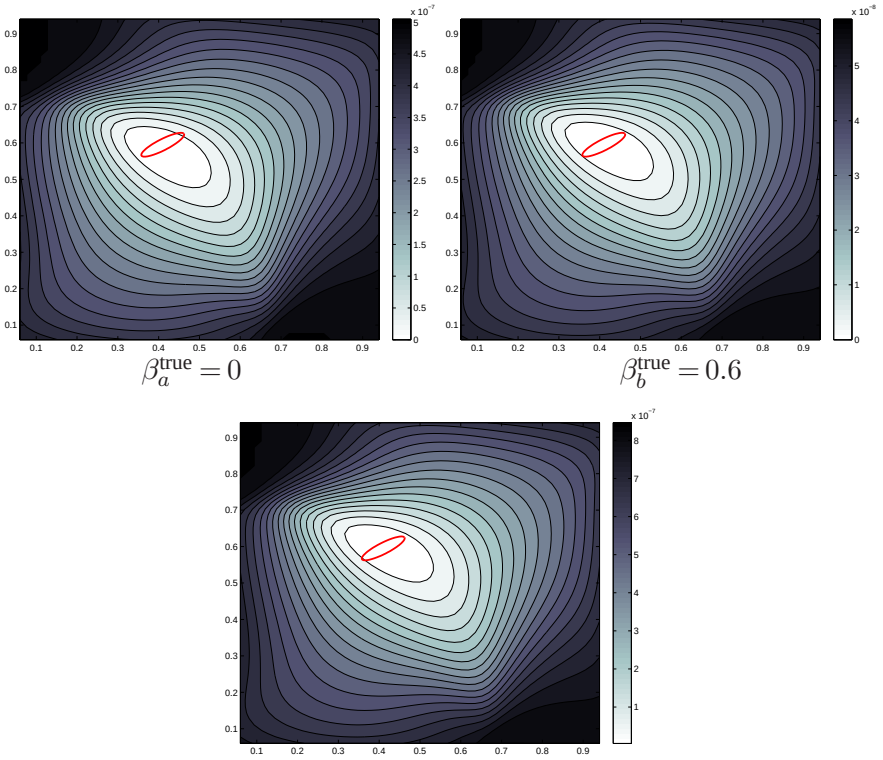

Figure 8: *Identification of inclusion 2 (elliptical): distribution of J^{min} over search grid* **G**, *and outline of true inclusion.*

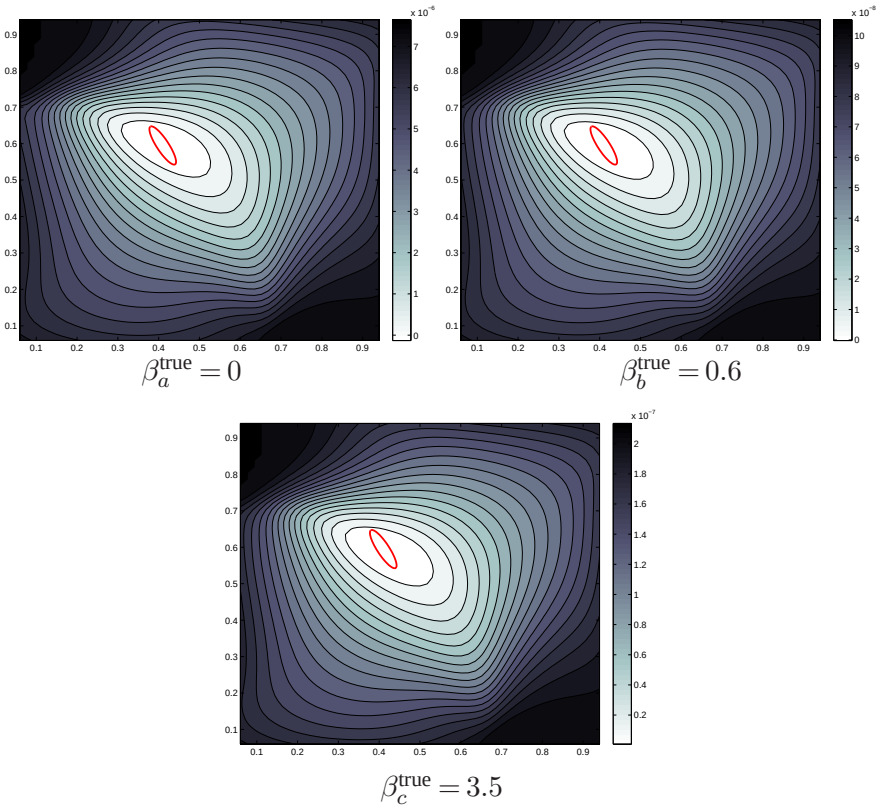

Figure 9: *Identification of inclusion 3 (elliptical): distribution of J^{min} over search grid* **G**, *and outline of true inclusion.*

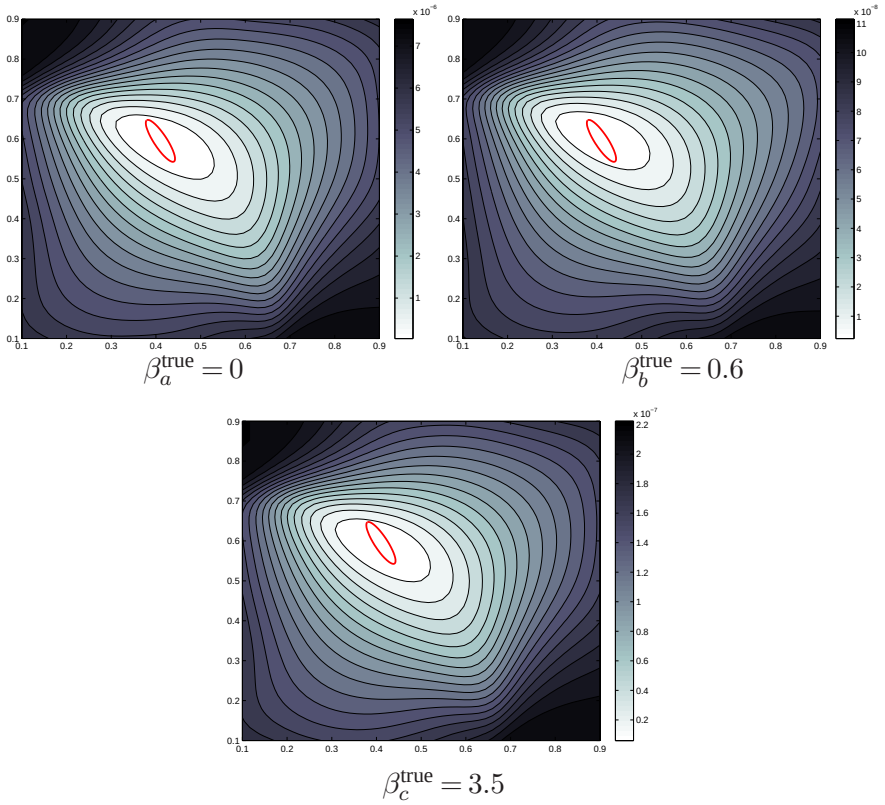

Figure 10: *Identification of inclusion 3 (elliptical): distribution of J^{min} over search grid* $\mathbf{G}$*, and outline of true inclusion (noisy data, with 20% noise on $u^{obs} - u$).*

where $C(\varepsilon, \beta)\boldsymbol{I} = \boldsymbol{\mathcal{A}}_{11}\varepsilon^2$, see (66). Figure 11 shows that $C(R^{\text{est}}(\beta), \beta)$ is, for this example, largely insensitive to the assumed value of β. This is consistent with other asymptotic approaches to inclusion identification which show that the main identifiable feature of small buried inclusions is their polarization tensor [24]. Moreover, an elementary calculation allows to show (again assuming a circular trial inclusion) that $J^{\min}(\boldsymbol{a})$ evaluated at a fixed sampling point $\boldsymbol{a}$ is either increasing or decreasing with β, i.e. is minimum w.r.t. β for either $\beta = 0$ (impenetrable inclusion) or $\beta = +\infty$.

Extending the approximate global search procedure proposed in this section to the identification of two (or more) inclusions is not straightforward, as one would have to either (i) consider all *pairs* of sampling points $(\boldsymbol{a}', \boldsymbol{a}'') \in \mathbf{G} \times \mathbf{G}$ (entailing a computing time proportional to the *square* of the search grid size), or (ii) define an alternating iterative method where one inclusion is sought at a time.

9 CONCLUSIONS

In this article, extending previous work on topological sensitivity, a methodology for expanding to order $O(\varepsilon^4)$ a generic cost function under the nucleation of a small inclusion of characteristic size ε has been developed, in the context of 2-D media characterized by a scalar conductivity coefficient. General formulae have been provided, where an adjoint solution is used to simplify the procedure through avoiding evaluation of higher-order topological sensitivities of field variables. Our approach

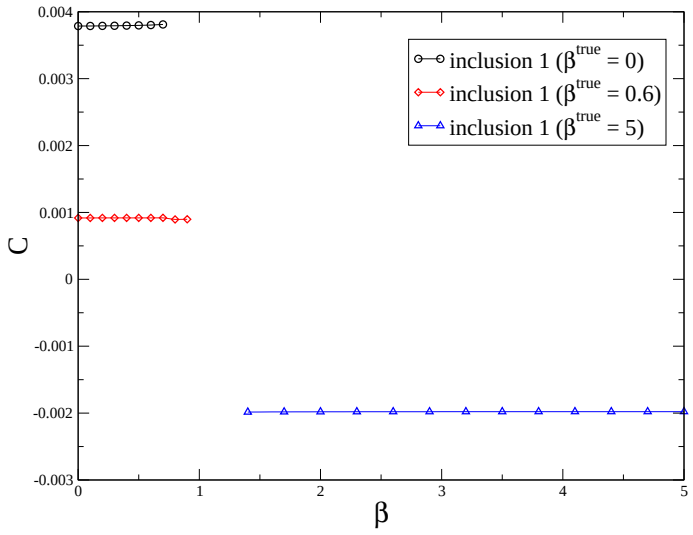

Figure 11: *Identification of hidden circular inclusion:* $C\big(R^{est}(\beta),\beta\big)$ *against* β *for inclusions 1a, 1b and 1c (noise-free data).*

was in particular shown to lead to useful computational strategies for computationally fast inclusion identification problems, in the form of a non-iterative fast approximate global search algorithm. The methodology used here is generic, and is therefore expected to yield similar expansions for other cases, e.g. penetrable elastic inclusions under static or dynamic conditions, which will be addressed in forthcoming investigations.

Appendix A EXACT SOLUTIONS

Let $\Omega = \{(r,\theta)\,\big|\,r<b\}$ (where (r,θ) are polar coordinates) denote the disk of radius b centered at the origin.

Green's functions for Dirichlet and Neumann problems. Define Green's functions $\mathcal{G}(\boldsymbol{x},\boldsymbol{\xi})$ by

$$\mathcal{G}(\boldsymbol{x},\boldsymbol{\xi}) = G(\boldsymbol{x},\boldsymbol{\xi}) + G_{\rm C}(\boldsymbol{x},\boldsymbol{\xi}), \qquad G_{\rm C}(\boldsymbol{x},\boldsymbol{\xi}) = \mp\frac{1}{2\pi}{\rm Log}\Big(\frac{1}{R}\frac{b}{\|\boldsymbol{x}\|}\Big), \tag{A.1}$$

where the '-' and '+' sign correspond to the cases $S_{\rm N}=S$, $S_{\rm D}=\emptyset$ ($\mathcal{G}=\mathcal{G}^{\rm N}$, Neumann) and $S_{\rm D}=S$, $S_{\rm N}=\emptyset$ ($\mathcal{G}=\mathcal{G}^{\rm D}$, Dirichlet), and with the definitions

$$r = \big\|\,\boldsymbol{\xi}-\boldsymbol{x}\,\big\|, \qquad R = \big\|\,\boldsymbol{\xi}-(b^2/\|\boldsymbol{x}\|^2)\boldsymbol{x}\,\big\|$$

The respective boundary conditions satisfied on $S=\{(r,\theta)\,\big|\,r=b\}$ by $\mathcal{G}^{\rm D}$ and $\mathcal{G}^{\rm N}$ are:

$$\mathcal{G}^{\rm D}(\boldsymbol{x},\boldsymbol{\xi}) = 0, \quad \mathcal{H}^{\rm N}(\boldsymbol{x},\boldsymbol{\xi}) = -\frac{1}{2\pi b} \qquad (\boldsymbol{\xi}\in S) \tag{A.2}$$

On evaluating analytically $\boldsymbol{\nabla}_x\boldsymbol{\nabla}_\xi G_{\rm C}$ and setting $\boldsymbol{x}=\boldsymbol{\xi}=\boldsymbol{a}$ for an arbitrary sampling point in Ω, one finds

$$\boldsymbol{\nabla}_x\boldsymbol{\nabla}_\xi G^{\rm D}_{\rm C}(\boldsymbol{a},\boldsymbol{a}) = -\boldsymbol{\nabla}_x\boldsymbol{\nabla}_\xi G^{\rm N}_{\rm C}(\boldsymbol{a},\boldsymbol{a}) = -\frac{1}{2\pi}\frac{b^2}{(b^2-\|\boldsymbol{a}\|^2)^2}\boldsymbol{I} \tag{A.3}$$

Potential and its small-inclusion expansion. Consider a circular inclusion B_ε located at the disk center, i.e. choose $\boldsymbol{a} = \mathbf{0}$ and set $B_\varepsilon = \{(r,\theta)\,\big|\, r < \varepsilon\}$. The solutions $u_\varepsilon^{(a,b,c,d)}$ of the Laplace transmission problem defined by (2), (4) with $B^\star = B_\varepsilon$ and respective boundary conditions

$$\begin{aligned} u_\varepsilon^{(a)} &= u_0\cos\theta \quad (\text{on } S), & k\boldsymbol{\nabla} u_\varepsilon^{(c)}\cdot\boldsymbol{n} &= (ku_0/b)\cos\theta \quad (\text{on } S),\\ u_\varepsilon^{(b)} &= u_0\cos 2\theta \quad (\text{on } S), & k\boldsymbol{\nabla} u_\varepsilon^{(d)}\cdot\boldsymbol{n} &= 2(ku_0/b)\cos 2\theta \quad (\text{on } S) \end{aligned} \tag{A.4}$$

are respectively given by

$$\begin{aligned} u_\varepsilon^{(a)} &= u_0\frac{(1+\eta)}{1+\eta\varepsilon^2/b^2}\,\frac{r}{b}\cos\theta, & u_\varepsilon^{(c)} &= u_0\frac{(1+\eta)}{1-\eta\varepsilon^2/b^2}\,\frac{r}{b}\cos\theta,\\ u_\varepsilon^{(b)} &= u_0\frac{(1+\eta)}{1+\eta\varepsilon^4/b^4}\,\frac{r^2}{b^2}\cos 2\theta, & u_\varepsilon^{(d)} &= u_0\frac{(1+\eta)}{1-\eta\varepsilon^4/b^4}\,\frac{r^2}{b^2}\cos 2\theta \end{aligned} \tag{A.5}$$

inside the inclusion, and by

$$\begin{aligned} u_\varepsilon^{(a)} &= u_0\frac{1+\eta\varepsilon^2/r^2}{1+\eta\varepsilon^2/b^2}\,\frac{r}{b}\cos\theta, & u_\varepsilon^{(c)} &= u_0\frac{1+\eta\varepsilon^2/r^2}{1-\eta\varepsilon^2/b^2}\,\frac{r}{b}\cos\theta,\\ u_\varepsilon^{(b)} &= u_0\frac{1+\eta\varepsilon^4/r^4}{1+\eta\varepsilon^4/b^4}\,\frac{r^2}{b^2}\cos 2\theta, & u_\varepsilon^{(d)} &= u_0\frac{1+\eta\varepsilon^4/r^4}{1-\eta\varepsilon^4/b^4}\,\frac{r^2}{b^2}\cos 2\theta \end{aligned} \tag{A.6}$$

in the surrounding medium, having put

$$\eta = \frac{1-\beta}{1+\beta}$$

The respective reference solutions u when there is no inclusion (defined up to an arbitrary additive constant for cases (c) and (d)) are characterized by

$$\begin{aligned} u^{(a,c)}(r,\theta) &= \frac{u_0 r}{b}\cos\theta, & u^{(b,d)}(r,\theta) &= \frac{u_0 r^2}{b^2}\cos 2\theta,\\ \boldsymbol{\nabla} u^{(a,c)}(\boldsymbol{a}) &= \frac{u_0}{b}\boldsymbol{e}_x, & \boldsymbol{\nabla} u^{(b,d)}(\boldsymbol{a}) &= \mathbf{0},\\ \boldsymbol{\nabla}^2 u^{(a,c)}(\boldsymbol{a}) &= \mathbf{0}, & \boldsymbol{\nabla}^2 u^{(b,d)}(\boldsymbol{a}) &= \frac{2u_0}{b^2}(\boldsymbol{e}_x\otimes\boldsymbol{e}_x - \boldsymbol{e}_y\otimes\boldsymbol{e}_y), \end{aligned} \tag{A.7}$$

where $\boldsymbol{e}_x, \boldsymbol{e}_y$ are unit vectors such that $\boldsymbol{\xi} = r(\cos\theta\boldsymbol{e}_x + \sin\theta\boldsymbol{e}_y)$.

Potential energy and its small-inclusion expansion. The potential energies for the respective problems are, together with their $O(\varepsilon^4)$ expansions, easily obtained from solutions (A.6) as

$$\mathcal{E}^{(a)}(B_\varepsilon) = \frac{k\pi u_0^2}{2}\frac{1-\eta\varepsilon^2/b^2}{1+\eta\varepsilon^2/b^2} = \frac{k\pi u_0^2}{2}\Big(1 - 2\eta\frac{\varepsilon^2}{b^2} + 2\eta^2\frac{\varepsilon^4}{b^4}\Big) + o(\varepsilon^4) \tag{A.8a}$$

$$\mathcal{E}^{(b)}(B_\varepsilon) = k\pi u_0^2\frac{1-\eta\varepsilon^4/b^4}{1+\eta\varepsilon^4/b^4} = k\pi u_0^2\Big(1 - 2\eta\frac{\varepsilon^4}{b^4}\Big) + o(\varepsilon^4) \tag{A.8b}$$

$$\mathcal{E}^{(c)}(B_\varepsilon) = -\frac{k\pi u_0^2}{2}\frac{1+\eta\varepsilon^2/b^2}{1-\eta\varepsilon^2/b^2} = -\frac{k\pi u_0^2}{2}\Big(1 + 2\eta\frac{\varepsilon^2}{b^2} + 2\eta^2\frac{\varepsilon^4}{b^4}\Big) + o(\varepsilon^4) \tag{A.8c}$$

$$\mathcal{E}^{(d)}(B_\varepsilon) = -k\pi u_0^2\frac{1+\eta\varepsilon^4/b^4}{1-\eta\varepsilon^4/b^4} = -k\pi u_0^2\Big(1 + 2\eta\frac{\varepsilon^4}{b^4}\Big) + o(\varepsilon^4) \tag{A.8d}$$

An evaluation of expressions (70a,b) of coefficients $\mathcal{T}_2, \mathcal{T}_4$ using (A.3) for $\boldsymbol{a} = \mathbf{0}$ together with formulae (A.7) yields $O(\varepsilon^4)$ expansions of $\mathcal{E}^{(a,b,c,d)}(B_\varepsilon)$ that are identical with (A.8a–d). These special

cases thus corroborate Proposition 3. Likewise, it is easy to check that the alternative formula (71) from [15] does not yield the correct value of the $O(\varepsilon^4)$ contribution to the expansion of $\mathcal{E}(B_\varepsilon)$ for cases (a,c) where the omitted contribution of $\boldsymbol{\nabla} u(\boldsymbol{a})\cdot\boldsymbol{\nabla}_x\boldsymbol{\nabla}_\xi G_{\mathrm{C}}(\boldsymbol{a},\boldsymbol{a})\cdot\boldsymbol{\nabla} u(\boldsymbol{a})$ is nonzero.

Appendix B DETERMINATION OF $\boldsymbol{\mathcal{U}}_1, \boldsymbol{\mathcal{U}}_2$ AND ASSOCIATED CONSTANT TENSORS

The vector and tensor functions $\boldsymbol{\mathcal{U}}_1, \boldsymbol{\mathcal{U}}_2, \boldsymbol{\mathcal{U}}_3$ introduced in Sec. 4.3 can be interpreted as solutions to transmission problems in infinite media containing a normalized penetrable inclusion, of the form

$$\begin{cases} k\Delta U = 0 & (\text{in } \mathbb{R}^2\setminus\mathscr{B}),\\ k^\star\Delta(U-U^0) = 0 & (\text{in } \mathscr{B}),\end{cases} \qquad \begin{cases} k(\boldsymbol{\nabla}U)_{\mathrm{m}}\cdot\boldsymbol{n} = k^\star\boldsymbol{\nabla}(U-U^0)_{\mathrm{i}}\cdot\boldsymbol{n} & (\text{on } \partial\mathscr{B}),\\ U_{\mathrm{m}} = U_{\mathrm{i}} & (\text{on } \partial\mathscr{B}),\\ U = O(\|\bar{\boldsymbol{\xi}}\|^{-1}) & (\|\bar{\boldsymbol{\xi}}\|\to\infty),\end{cases} \tag{B.1}$$

where U^0, analogous to a prescribed initial strain in elasticity, is given on $\mathscr{B}$. To establish this interpretation, one first establishes the weak formulation

$$\mathcal{A}(U,W) = \int_{\mathscr{B}} \beta k\boldsymbol{\nabla}U^0\cdot\boldsymbol{\nabla}W\ \mathrm{d}V, \tag{B.2}$$

with the bilinear form $\mathcal{A}(\cdot,\cdot)$ defined for trial functions W continuous across $\partial\mathscr{B}$ by

$$\mathcal{A}(U,W) = \int_{\mathbb{R}^2\setminus\mathscr{B}} k\boldsymbol{\nabla}U\cdot\boldsymbol{\nabla}W\ \mathrm{d}V + \int_{\mathscr{B}} \beta k\boldsymbol{\nabla}\tilde{U}\cdot\boldsymbol{\nabla}W\ \mathrm{d}V \tag{B.3}$$

and with $\beta = k^\star/k$, by means of the following steps: (i) multiply the field equations in (B.1) by a trial function W (assumed to be continuous across $\partial\mathscr{B}$ and to suitably decay at infinity), (ii) integrate the resulting identities by parts, (iii) add them and (iv) invoke the transmission conditions in (B.1).

Next, setting $W = G(\bar{\boldsymbol{x}},\cdot)$ with $\bar{\boldsymbol{x}}\in\mathscr{B}$, one finds the identity

$$\int_{\mathbb{R}^2\setminus\mathscr{B}} k\boldsymbol{\nabla}U\cdot\boldsymbol{\nabla}G(\bar{\boldsymbol{x}},\cdot)\ \mathrm{d}V + \int_{\mathscr{B}} k\boldsymbol{\nabla}\tilde{U}\cdot\boldsymbol{\nabla}G(\bar{\boldsymbol{x}},\cdot)\ \mathrm{d}V = U(\bar{\boldsymbol{x}}) \qquad (\bar{\boldsymbol{x}}\in\mathscr{B})$$

by (i) integrating by parts via the divergence theorem, (ii) exploiting the field equation $k\Delta G(\bar{\boldsymbol{x}},\cdot) + \delta(\cdot-\bar{\boldsymbol{x}})$ verified by the full-space Green's function and (iii) invoking the continuity between U and $\tilde{U}$ on $\partial\mathscr{B}$. On setting $W = G(\bar{\boldsymbol{x}},\cdot)$ and substituting the above identity into (B.2), one therefore finds that $\tilde{U}$ is governed by the integral equation

$$U(\bar{\boldsymbol{x}}) - (1-\beta)k\int_{\mathscr{B}} \boldsymbol{\nabla}\tilde{U}(\bar{\boldsymbol{\xi}})\cdot\boldsymbol{\nabla}G(\bar{\boldsymbol{x}},\bar{\boldsymbol{\xi}})\ \mathrm{d}\bar{V}_{\bar{\xi}} = \beta\int_{\mathscr{B}} \boldsymbol{\nabla}U^0(\bar{\boldsymbol{\xi}})\cdot\boldsymbol{\nabla}G(\bar{\boldsymbol{x}},\bar{\boldsymbol{\xi}})\ \mathrm{d}\bar{V}_{\bar{\xi}} \qquad (\bar{\boldsymbol{x}}\in\mathscr{B}). \tag{B.4}$$

The governing integral equations (49a–c) for $\boldsymbol{\mathcal{U}}_1, \boldsymbol{\mathcal{U}}_2, \boldsymbol{\mathcal{U}}_3$ are then seen to be of the form (B.4) with

$$U^0(\bar{\boldsymbol{\xi}}) = \frac{1-\beta}{\beta}\bar{\boldsymbol{\xi}}, \qquad U^0(\bar{\boldsymbol{\xi}}) = \frac{1-\beta}{2\beta}\bar{\boldsymbol{\xi}}\otimes\bar{\boldsymbol{\xi}}, \qquad U^0(\bar{\boldsymbol{\xi}}) = \frac{1-\beta}{3\beta}\bar{\boldsymbol{\xi}}\otimes\bar{\boldsymbol{\xi}}\otimes\bar{\boldsymbol{\xi}}, \tag{B.5}$$

respectively (using tensor notation).

Determination of $\mathcal{U}_1, \mathcal{U}_2, \mathcal{U}_3$ for circular inclusions. One approach for determining auxiliary solutions $\mathcal{U}_1, \mathcal{U}_2, \mathcal{U}_3$ consists in using separation of variables in polar coordinates directly in the set (B.1) of field equations and transmission conditions, with U^0 given by (B.5). Expressions (65a,b) and (67) are then found after some straightforward manipulation.

Alternatively, elementary analytical integration manipulations yield formulae

$$\big[\bar{\mathcal{L}}\bar{\boldsymbol{\xi}}\big](\bar{\boldsymbol{x}}) = \frac{1-\beta}{2}\bar{\boldsymbol{x}}, \tag{B.6a}$$

$$\big[\bar{\mathcal{L}}(\bar{\boldsymbol{\xi}}\otimes\bar{\boldsymbol{\xi}})\big](\bar{\boldsymbol{x}}) = \frac{1-\beta}{2}\Big[\,\bar{\boldsymbol{x}}\otimes\bar{\boldsymbol{x}} + \frac{1}{2}(\|\bar{\boldsymbol{x}}\|-2)\boldsymbol{I}\,\Big], \tag{B.6b}$$

$$\big[\bar{\mathcal{L}}(\bar{\boldsymbol{\xi}}\otimes\bar{\boldsymbol{\xi}}\otimes\bar{\boldsymbol{\xi}})\big](\bar{\boldsymbol{x}}) = \frac{1-\beta}{2}\Big[\,\bar{\boldsymbol{x}}\otimes\bar{\boldsymbol{x}}\otimes\bar{\boldsymbol{x}} + \frac{1}{4}(\|\bar{\boldsymbol{x}}\|-1)\boldsymbol{\mathcal{K}}(\bar{\boldsymbol{x}})\,\Big] \tag{B.6c}$$

(with $\boldsymbol{\mathcal{K}}(\bar{\boldsymbol{x}})$ defined as in (67)) which then allow direct verification of the fact that expressions (65a,b) and (67) satisfy equations (49a-c).

Appendix C THE CASE OF A CENTRALLY-SYMMETRIC INCLUSION

When $\mathscr{B}$ has central symmetry (i.e. if $\bar{\boldsymbol{\xi}}\in\mathscr{B} \Leftrightarrow -\bar{\boldsymbol{\xi}}\in\mathscr{B}$), the constant tensor $\boldsymbol{\mathcal{A}}_{12}$ defined by (51b) vanishes. Denoting by $\sigma:\ \bar{\boldsymbol{\xi}}\to\sigma\bar{\boldsymbol{\xi}} \coloneqq -\bar{\boldsymbol{\xi}}$ the central-symmetry linear mapping, let $\mathscr{B}=\bar{\mathscr{B}}'\cup\bar{\mathscr{B}}''$, with $\mathscr{B}''=\sigma\mathscr{B}'$ and $\mathscr{B}'\cap\mathscr{B}''=\emptyset$. The mapping σ is in particular such that

$$\mathrm{d}V(\sigma\bar{\boldsymbol{\xi}}) = \mathrm{d}V(\bar{\boldsymbol{\xi}}) \tag{C.1}$$

Lemma 7. *Solution $\boldsymbol{\mathcal{U}}_2$ is symmetric: $\boldsymbol{\mathcal{U}}_2(\sigma\bar{\boldsymbol{\xi}}) = \boldsymbol{\mathcal{U}}_2(\bar{\boldsymbol{\xi}})$.*

Remark 5. *By virtue of Lemma 7, one has $\bar{\boldsymbol{\nabla}}\boldsymbol{\mathcal{U}}_2(\sigma\bar{\boldsymbol{\xi}}) = -\bar{\boldsymbol{\nabla}}\boldsymbol{\mathcal{U}}_2(\bar{\boldsymbol{\xi}})$ and*

$$\boldsymbol{\mathcal{A}}_{12} = \int_{\mathscr{B}} \bar{\boldsymbol{\nabla}}\boldsymbol{\mathcal{U}}_2(\bar{\boldsymbol{\xi}})\, d\bar{V}_{\bar{\xi}} = \int_{\mathscr{B}'} [\bar{\boldsymbol{\nabla}}\boldsymbol{\mathcal{U}}_2(\bar{\boldsymbol{\xi}}) + \bar{\boldsymbol{\nabla}}\boldsymbol{\mathcal{U}}_2(\sigma\bar{\boldsymbol{\xi}})]\, d\bar{V}_{\bar{\xi}} = \boldsymbol{0}$$

Proof. Let $\boldsymbol{\mathcal{U}}_2^{\text{even}}$ and $\boldsymbol{\mathcal{U}}_2^{\text{odd}}$, the even and odd parts of $\boldsymbol{\mathcal{U}}_2$, be defined by:

$$\boldsymbol{\mathcal{U}}_2^{\text{even}}(\bar{\boldsymbol{\xi}}) = \frac{1}{2}\big(\boldsymbol{\mathcal{U}}_2(\bar{\boldsymbol{\xi}}) + \boldsymbol{\mathcal{U}}_2(\sigma\bar{\boldsymbol{\xi}})\big)\,, \qquad \boldsymbol{\mathcal{U}}_2^{\text{odd}}(\bar{\boldsymbol{\xi}}) = \frac{1}{2}\big(\boldsymbol{\mathcal{U}}_2(\bar{\boldsymbol{\xi}}) - \boldsymbol{\mathcal{U}}_2(\sigma\bar{\boldsymbol{\xi}})\big) \tag{C.2}$$

These definitions imply that

$$\boldsymbol{\mathcal{U}}_2^{\text{even}}(\sigma\bar{\boldsymbol{\xi}}) = \boldsymbol{\mathcal{U}}_2^{\text{even}}(\bar{\boldsymbol{\xi}})\,, \qquad \boldsymbol{\mathcal{U}}_2^{\text{odd}}(\sigma\bar{\boldsymbol{\xi}}) = -\boldsymbol{\mathcal{U}}_2^{\text{odd}}(\bar{\boldsymbol{\xi}}) \tag{C.3}$$

$$\bar{\boldsymbol{\nabla}}\boldsymbol{\mathcal{U}}_2^{\text{even}}(\sigma\bar{\boldsymbol{\xi}}) = -\bar{\boldsymbol{\nabla}}\boldsymbol{\mathcal{U}}_2^{\text{even}}(\bar{\boldsymbol{\xi}})\,, \qquad \bar{\boldsymbol{\nabla}}\boldsymbol{\mathcal{U}}_2^{\text{odd}}(\sigma\bar{\boldsymbol{\xi}}) = \bar{\boldsymbol{\nabla}}\boldsymbol{\mathcal{U}}_2^{\text{odd}}(\bar{\boldsymbol{\xi}}) \tag{C.4}$$

Now, on inserting the decomposition $\boldsymbol{\mathcal{U}}_2 = \boldsymbol{\mathcal{U}}_2^{\text{even}} + \boldsymbol{\mathcal{U}}_2^{\text{odd}}$ in integral equation (49b), writing the resulting equations for a pair of symmetrical collocation points $\bar{\boldsymbol{x}}$ and $\sigma\bar{\boldsymbol{x}}$ ($\bar{\boldsymbol{x}}\in\mathscr{B}'$), using property (C.4), and noting that the distance function and the fundamental solution $G(\bar{\boldsymbol{x}},\bar{\boldsymbol{\xi}})$ defined by (38) satisfy

$$\|\sigma\bar{\boldsymbol{x}} - \bar{\boldsymbol{\xi}}\| = \|\bar{\boldsymbol{x}} - \sigma\bar{\boldsymbol{\xi}}\|\,, \qquad \bar{\boldsymbol{\nabla}}G(\sigma\bar{\boldsymbol{x}},\bar{\boldsymbol{\xi}}) = -\bar{\boldsymbol{\nabla}}G(\bar{\boldsymbol{x}},\sigma\bar{\boldsymbol{\xi}})$$

the following pair of integral equations is arrived at:

$$\begin{aligned}
\big[(\mathcal{I}-\bar{\mathcal{L}}^{\text{even}}_{\mathscr{B}'})\,\boldsymbol{\mathcal{U}}^{\text{even}}_2\big](\bar{\boldsymbol{x}}) - \big[\bar{\mathcal{L}}^{\text{odd}}_{\mathscr{B}'}\,\boldsymbol{\mathcal{U}}^{\text{odd}}_2\big](\bar{\boldsymbol{x}}) &= \frac{1}{2}\big[\bar{\mathcal{L}}^{\text{even}}_{\mathscr{B}'}(\bar{\boldsymbol{\xi}}\otimes\bar{\boldsymbol{\xi}})\big](\bar{\boldsymbol{x}}) \\
\big[(\mathcal{I}-\bar{\mathcal{L}}^{\text{even}}_{\mathscr{B}'})\,\boldsymbol{\mathcal{U}}^{\text{even}}_2\big](\bar{\boldsymbol{x}}) + \big[\bar{\mathcal{L}}^{\text{odd}}_{\mathscr{B}'}\,\boldsymbol{\mathcal{U}}^{\text{odd}}_2\big](\bar{\boldsymbol{x}}) &= \frac{1}{2}\big[\bar{\mathcal{L}}^{\text{even}}_{\mathscr{B}'}(\bar{\boldsymbol{\xi}}\otimes\bar{\boldsymbol{\xi}})\big](\bar{\boldsymbol{x}})
\end{aligned} \qquad (\bar{\boldsymbol{x}}\in\mathscr{B}') \qquad \text{(C.5)}$$

with the definitions

$$\big[\bar{\mathcal{L}}^{\text{even}}_{\mathscr{B}'}f\big](\bar{\boldsymbol{x}}) = \big[\bar{\mathcal{L}}_{\mathscr{B}'}f\big](\bar{\boldsymbol{x}}) + \big[\bar{\mathcal{L}}_{\mathscr{B}'}f\big](\sigma\bar{\boldsymbol{x}}) \qquad \big[\bar{\mathcal{L}}^{\text{odd}}_{\mathscr{B}'}f\big](\bar{\boldsymbol{x}}) = \big[\bar{\mathcal{L}}_{\mathscr{B}'}f\big](\bar{\boldsymbol{x}}) - \big[\bar{\mathcal{L}}_{\mathscr{B}'}f\big](\sigma\bar{\boldsymbol{x}})$$

On taking the difference of equations (C.5), one obtains

$$\big[\bar{\mathcal{L}}^{\text{odd}}_{\mathscr{I}'}\,\boldsymbol{\mathcal{U}}^{\text{odd}}_2\big](\bar{\boldsymbol{x}}) = 0$$

Hence, $\boldsymbol{\mathcal{U}}^{\text{odd}}_2(\bar{\boldsymbol{\xi}}) = 0$, i.e. $\boldsymbol{\mathcal{U}}_2$ has the desired symmetry. □

REFERENCES

[1] KLEIBER, M. E. A. *Parameter Sensitivity in Nonlinear Mechanics: Theory and Finite Element Computations.* J. Wiley and Sons, New York (1997).

[2] SOKOLOWSKI, J., ZOLESIO, J. P. *Introduction to shape optimization. Shape sensitivity analysis*, vol. 16 of *Springer series in Computational Mathematics*. Springer-Verlag (1992).

[3] ESCHENAUER, H. A., KOBELEV, V. V., SCHUMACHER, A. Bubble method for topology and shape optimization of structures. *Structural Optimization*, **8**:42–51 (1994).

[4] SCHUMACHER, A. *Topologieoptimierung von Bauteilstrukturen unter Verwendung von Lochpositionierungskriterien*. Ph.D. thesis, Univ. of Siegen, Germany (1995).

[5] GARREAU, S., GUILLAUME, P., MASMOUDI, M. The topological asymptotic for PDE systems: the elasticity case. *SIAM J. Contr. Opt.*, **39**:1756–1778 (2001).

[6] GUZINA, B. B., BONNET, M. Topological derivative for the inverse scattering of elastic waves. *Quart. J. Mech. Appl. Math.*, **57**:161–179 (2004).

[7] BONNET, M., GUZINA, B. B. Sounding of finite solid bodies by way of topological derivative. *Int. J. Num. Meth. in Eng.*, **61**:2344–2373 (2004).

[8] GUZINA, B. B., CHIKICHEV, I. From imaging to material identification: a generalized concept of topological sensitivity. *J. Mech. Phys. Solids*, **55**:245–279 (2007).

[9] MALCOLM, A., GUZINA, B. On the topological sensitivity of transient acoustic fields. *Wave Motion*, **45**:821–834 (2008).

[10] FEIJÓO, G. R. A new method in inverse scattering based on the topological derivative. *Inverse Problems*, **20**:1819–1840 (2004).

[11] MASMOUDI, M., POMMIER, J., SAMET, B. The topological asymptotic expansion for the Maxwell equations and some applications. *Inverse Problems*, **21**:547–564 (2005).

[12] BONNET, M. Inverse acoustic scattering by small-obstacle expansion of misfit function. *Inverse Problems*, **24**:035022 (2008).

[13] AMMARI, H., KANG, H. *Reconstruction of small inhomogeneities from boundary measurements*. Lecture Notes in Mathematics 1846. Springer-Verlag (2004).

[14] AMSTUTZ, S. Sensitivity analysis with respect to a local perturbation of the material property. *Asymptotic Analysis*, **49**:87–108 (2006).

[15] ROCHA DE FARIA, J., NOVOTNY, A. A., FEIJÓO, R. A., TAROCO, E., PADRA, C. Second order topological sensitivity analysis. *Int. J. Solids Struct.*, **44**:4958–4977 (2007).

[16] BONNET, M. Discussion of "Second order topological sensitivity analysis" by J. Rocha de Faria et al. *Int. J. Solids Struct.*, **45**:705–707 (2008).

[17] ROCHA DE FARIA, J., NOVOTNY, A. A., FEIJÓO, R. A., TAROCO, E., PADRA, C. Response to the discussion of "Second order topological sensitivity analysis" by M. Bonnet. *Int. J. Solids Struct.*, **45**:708–711 (2008).

[18] MICHALEWICZ, Z., FOGEL, D. B. *How to solve it: modern heuristics*. Springer-Verlag (2004).

[19] TARANTOLA, A. *Inverse problem theory and methods for model parameter estimation*. SIAM (2005).

[20] CEDIO-FENGYA, D. J., MOSKOW, S., VOGELIUS, M. Identification of conductivity imperfections of small diameter by boundary measurements. Continuous dependence and computational reconstruction. *Inverse Problems*, **14**:553–595 (1998).

[21] BONNET, M. *Boundary Integral Equations Methods for Solids and Fluids*. John Wiley and Sons (1999).

[22] CHEN, G., ZHOU, J. *Boundary element methods*. Academic Press (1992).

[23] CÉA, J., GARREAU, S., GUILLAUME, P., MASMOUDI, M. The shape and topological optimization connection. *Comp. Meth. Appl. Mech. Engng.*, **188**:703–726 (2001).

[24] AMMARI, H., KANG, H. Generalized polarization tensors, inverse conductivity problems, and dilute composite materials: a review. *Contemp. Math.*, **408**:1–67 (2006).